



**HAL**  
open science

# Neutral 2-phenylbenzimidazole-based iridium( iii ) complexes with picolinate ancillary ligand: tuning the emission properties by manipulating the substituent on the benzimidazole ring

Emiliano Martínez-Vollbert, Christian Philouze, Théo Cavnac, Camille Latouche, Frédérique Loiseau, Pierre-Henri Lanoë

## ► To cite this version:

Emiliano Martínez-Vollbert, Christian Philouze, Théo Cavnac, Camille Latouche, Frédérique Loiseau, et al.. Neutral 2-phenylbenzimidazole-based iridium( iii ) complexes with picolinate ancillary ligand: tuning the emission properties by manipulating the substituent on the benzimidazole ring. Dalton Transactions, 2024, 53 (10), pp.4705-4718. 10.1039/D3DT03498D . hal-04548781

**HAL Id: hal-04548781**

**<https://hal.science/hal-04548781v1>**

Submitted on 29 Jul 2024

**HAL** is a multi-disciplinary open access archive for the deposit and dissemination of scientific research documents, whether they are published or not. The documents may come from teaching and research institutions in France or abroad, or from public or private research centers.

L'archive ouverte pluridisciplinaire **HAL**, est destinée au dépôt et à la diffusion de documents scientifiques de niveau recherche, publiés ou non, émanant des établissements d'enseignement et de recherche français ou étrangers, des laboratoires publics ou privés.

# Neutral 2-phenylbenzimidazole-based iridium(III) complexes with picolinate ancillary ligand: Tuning the emission properties by handling the substituent on the benzimidazole ring

Received 00th January 20xx,  
Accepted 00th January 20xx

DOI: 10.1039/x0xx00000x

Emiliano Martínez-Vollbert,<sup>a</sup> Christian Philouze,<sup>a</sup> Théo Cavignac,<sup>b</sup> Camille Latouche,<sup>b,c,†</sup> Frédérique Loiseau,<sup>\*a</sup> Pierre-Henri Lanoë<sup>\*a</sup>

**Abstract:** We report the synthesis and characterization of ten neutral bisheteroleptic iridium(III) complexes with 2-phenylbenzimidazole cyclometallating ligand and picolinate as ancillary ligand. The 2-phenylbenzimidazole has been modified by selected substituents introduced on the cyclometallating ring and/or on the benzimidazole moiety. The integrity of the complexes has been assessed by NMR spectroscopy, by high resolution mass spectrometry and by elemental analysis. The complexes demonstrated to be highly phosphorescent at room temperature and the throughout luminescence study with comprehensive *ab initio* calculations allow us to determine the lowest emitting existed state which depends on the substituent nature and position on the cyclometallating ligand.

## Introduction

Organic Light Emitting Diodes (OLEDs) and Light-Emitting Electrochemical Cells (LEECs) represent very interesting technologies for lighting displays as such devices are able to work at low voltage.<sup>1–3</sup> In these technologies, the excitons generated by the recombination of the injected holes and electrons are both in singlet and triplet excited states, with the ratio 1:3 making the theoretical External Quantum Efficiency (EQE) of only 25% for pure organic devices that can emit solely from the singlet excited state. The seminal work of Thompson and Forrest has demonstrated that phosphorescent emitters are able to convert the singlet exciton to triplet one, therefore offering the possibility to harvest 100% of the exciton and raise the theoretical EQE to the unity.<sup>4–6</sup> Thus, since the early 2000's the search of highly emissive and color-tunable transition metal based emitters has known an impressive booming. Among the transition metal complexes, two metals display terrific potentials in lighting displays with complexes displaying very high quantum yields, relatively short lifetimes and high emission energy tunability, being the octahedral Ir(III) and the square planar Pt(II).<sup>7</sup> Those emission properties have been brought to light thanks to the cyclometallation. Indeed, the metal-carbon bond with the strong  $\sigma$  donor ability from C, along with the  $\pi$ -acceptor ability of the pyridine, gives a very strong ligand field to these metals, leading to the upon mentioned tremendous photophysical properties of the lowest excited state. Consequently, cyclometallated Ir(III) and Pt(II) complexes are studied or used in numerous applications, spanning from triplet emitters in electroluminescent devices,<sup>3,12–17</sup> sensors,<sup>18–22</sup> theragnostic and/or therapeutic

agents,<sup>23–28</sup> to photosensitizers and photocatalysts<sup>18,29,30</sup> to name few examples.

The neutral Ir(III) complexes have been particularly studied and can be divided in three main types being: the tris-heteroleptic *fac/mer*-Ir(C<sup>N</sup>)<sub>3</sub>, where C is a cyclometallated carbon and N is a heterocyclic nitrogen; the bis-heteroleptic Ir(C<sup>N</sup>)<sub>2</sub>(LX), where LX represents an anionic ancillary ligand and tris-heteroleptic of the form Ir(N<sup>^</sup>C<sup>N</sup>)(C<sup>N</sup>)X, where X is an anionic ligand typically a chloride<sup>9,10,31,32</sup>. The emission properties of Ir(III) complexes are often an intriguing interplay of emissive excited states, taking as the reference the well-known *fac*-Ir(ppy)<sub>3</sub> (hereafter denoted simply Ir(ppy)<sub>3</sub>, ppy = 2-phenylpyridine). The lowest-energy absorption is of <sup>1</sup>MLCT (metal-to-ligand charge transfer) nature and likewise the emissive level is recognized to be of <sup>3</sup>MLCT nature ( $\lambda_{em} = 508$  nm,  $\tau = 1.6$   $\mu$ s in MeTHF at r.t.).<sup>36,37</sup> Higher-lying excited states of <sup>3</sup>IL (intra-ligand or ligand centred) nature are also present and in several cases the energy separation with the triplet MLCT excited state is rather thin or even "inverted", <sup>3</sup>IL being the lowest excited state. This is the case for the heteroleptic complex (thpy)<sub>2</sub>Ir(acac) (thpy = thienylpyridine, acac = acetylacetonate) displaying an r.t. emission at  $\lambda_{em} = 562$  nm with  $\tau = 5.3$   $\mu$ s in MeTHF, which is recognized to be a genuine <sup>3</sup>IL emitter.<sup>10</sup> In addition, the lowest lying excited state of bis-

<sup>a</sup> E. Martínez-Vollbert, Dr. C. Philouze, Pr. F. Loiseau, Dr. P.-H. Lanoë, Univ. Grenoble Alpes, CNRS, DCM, 38000 Grenoble, France Mail: frederique.loiseau@univ-grenoble-alpes.fr, pierre-henri.lanoë@univ-grenoble-alpes.fr

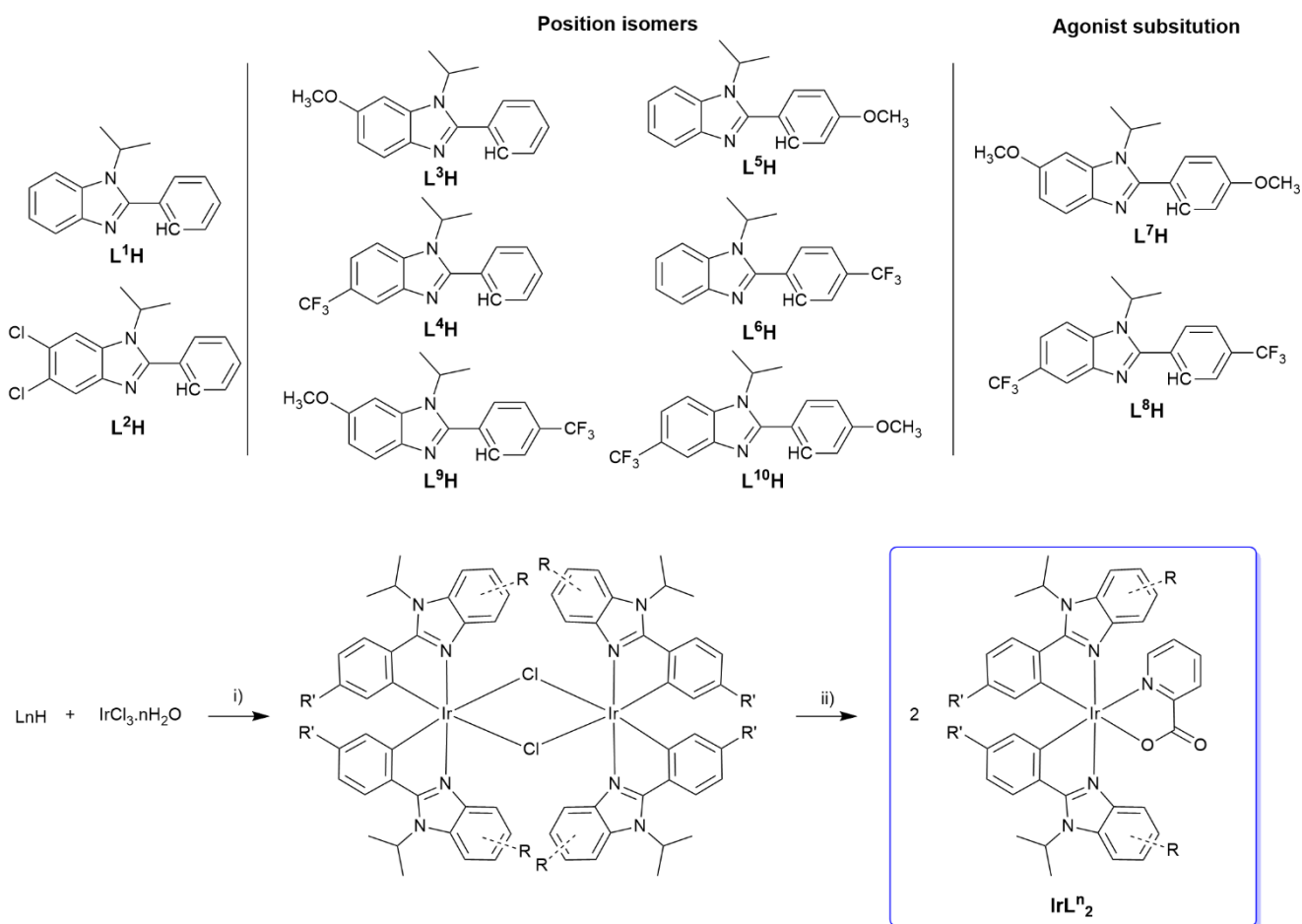
<sup>b</sup> T. Cavignac, Dr. C. Latouche Université de Nantes, CNRS, Institut des Matériaux Jean Rouxel, IMN, F-44000 Nantes, France

<sup>c</sup> Insitut universitaire de France (IUF)

† Corresponding author for the calculation studies Mail: camille.latouche@cnrs-imn.fr

Electronic Supplementary Information (ESI) available: [details of any supplementary information available should be included here]. See DOI: 10.1039/x0xx00000x

## Cyclometallating ligands:



Scheme 1: Top, proligand structures. Bottom, synthesis of the complexes i) EtOEtOH/H<sub>2</sub>O reflux; ii) 2-picolinic acid, Na<sub>2</sub>C<sub>2</sub>O<sub>3</sub> 100 °C.

heteroleptic Ir(III) complexes can also be the ligand-to-ligand charge transfer (<sup>3</sup>LL'CT, L' = ancillary ligands) excited state. The <sup>3</sup>CT states radiative deactivation results in a broad emission profile and go along with a rigidochromism effect at low temperature (hypsochromic shift), while the <sup>3</sup>IL radiative deactivation results in a structured emission profile and no rigidochromism is observed and even a bathochromic shift can be observed.<sup>16,38–41</sup> In addition, the nature of the emitting excited states will also affect the radiative constant (*k<sub>r</sub>*), which is typically of the order of  $2 \times 10^5 \text{ s}^{-1}$  when the emission emanates from <sup>3</sup>MLCT/<sup>3</sup>LL'CT excited state and lower in the case of the <sup>3</sup>IL phosphorescence.<sup>41,42</sup> However, frequently cyclometallated Ir(III) complexes demonstrate an emission being a mixture of the <sup>3</sup>MLCT-<sup>3</sup>LC excited states.

The majority of the reported Ir(III) complexes, so do the Pt(II) ones, are derived directly from the introduction of substituent(s) on the 2-phenylpyridine ligand, and their photophysical properties are well established. On another hand, complexes based on 2-phenylbenzimidazole as cyclometallating ligand represent a smaller family, but are not devoid of interests. Numerous host materials for phosphors are based on benzimidazole heterocycles for OLEDs regarding their good electron mobility with excellent thermal stability.<sup>43–46</sup> From a synthesis point of view, this ligand is an attractive

scaffold for cyclometallating ligands, as it presents three divergence points which can be independently modified: the introduction of alkyl or aryl can be performed on the secondary amine, on the phenyl ring or on the benzimidazole ring, and the synthesis does not require the use of palladium-catalysed cross-coupling reactions.<sup>47,48</sup> Fine tuning of the emission properties has been achieved by the introduction of electron withdrawing/donating groups on the cyclometallating arene,<sup>46,49,58–61,50–57</sup> while the modification of the benzimidazole moiety has been performed by ring expansion.<sup>62</sup> For example, the introduction of -OCH<sub>3</sub> and CN groups on the cyclometallating phenyl ring allowed to tune the luminescence from 496 nm to 605 nm with quantum yield from 0.05 to unity.<sup>52</sup> Recently, we focused our effort toward the modification of this moiety by the introduction of chosen substituents leading to highly emissive cationic Ir(III) complexes and the luminescence and electrochemical properties have been successfully tuned.<sup>63</sup> In addition, we demonstrated that two complexes had the nature of their emitting excited state sensitive to the solvent polarity and it was possible to switch from <sup>3</sup>M/LLCT\* to <sup>3</sup>LC\*. Herein, we report a series of neutral Ir(III) complexes featuring 2-phenylbenzimidazole cyclometallating (N<sup>^C</sup>) ligand and picolinate as ancillary ligand. The N<sup>^C</sup> ligands (Scheme 1) are

designed to study the influence of the substituents (Cl, CF<sub>3</sub>, and OCH<sub>3</sub>) electron withdrawing/donating ability by playing on their localization on the ligand, on either the phenyl or the benzimidazole, or both through the synthesis of position isomers. It must be emphasized that the HOMO is usually localized on the Ir-ph moiety and the LUMO on the benzimidazole moiety.<sup>49,61</sup> The experimental data are successively confronted to state-of-the-art computational methods leading to unambiguous attribution of the emitting exciting state.

## Results and discussion

### Synthesis and characterization

The cyclometallating ligands (**HL<sup>n</sup>**, Scheme 1) and the  $\mu$ -dichloridodimers were synthesized following our previous report.<sup>64</sup> The ten new complexes **IrL<sup>n</sup><sub>2</sub>** were obtained by reacting an excess of picolinic acid with the adequate  $\mu$ -dichloridodimer in the presence of sodium bicarbonate in a mixture of 2-ethoxyethanol/water at 100°C overnight. After precipitation by water adjunction and filtration, the solids were purified by flash column chromatography on silica gel using mixtures of dichloromethane/methanol/triethylamine as eluent. All the complexes were characterized by <sup>1</sup>H, <sup>13</sup>C and <sup>19</sup>F (when applicable) NMR, by HRMS and elemental analysis. Crystallographic quality single crystals of **IrL<sup>6</sup><sub>2</sub>**, **IrL<sup>9</sup><sub>2</sub>** and **IrL<sup>10</sup><sub>2</sub>** have been obtained by slow vapor diffusion of diethyl ether or pentane in a concentrated solution of complex in dichloromethane. The cell parameters of each complex are summarized in table S1 and selected bond lengths and angles of the three complexes are presented in Table 1, along with the ones of complex [Ir(ppy)<sub>2</sub>pic]<sup>65</sup> for comparison purpose. The crystallization space groups and Bravais lattices are monoclinic P2<sub>1</sub>/m for **IrL<sup>6</sup><sub>2</sub>** and **IrL<sup>9</sup><sub>2</sub>**, and triclinic P-1 for **IrL<sup>10</sup><sub>2</sub>**. Each asymmetric unit displays a single complex; four complexes are present in the unit cell for **IrL<sup>6</sup><sub>2</sub>** and **IrL<sup>9</sup><sub>2</sub>** and two in the case of **IrL<sup>10</sup><sub>2</sub>**. As expected, we observed in the lattice the two  $\Delta$  and  $\Lambda$  isomers which arise from the reaction of the picolinate with the  $\mu$ -dichlorido-bridged Ir dimer having the *D*<sub>2</sub> symmetric  $\Delta\Delta$  and  $\Lambda\Lambda$  racemic mixture, where the two

C<sup>^</sup>N ligands have a cis-C,C and trans-N,N configuration around the metal center.<sup>66–68</sup> The resulting configuration for the three complexes is the expected *mer*-N3 cis-C,C trans-N,N within the two  $\Delta$  and  $\Lambda$  isomers. The reason for this outcome is due to the Ir–Ir distances rather small below 4 Å, which lead to important steric hindrance and to the so called *trans* effect of the Ir–C bonds, which induces preferential labilization of the bonds located in *trans*. It results in the stereochemical positioning of Ir–C and Ir–N bonds *trans* to one another.<sup>9,66</sup> The Ir–C and Ir–N<sub>C<sup>^</sup>N</sub> bond lengths displayed by the three complexes are similar, ranging from 1.995 to 2.020 Å, and so do the bond angles around the Ir core. The *trans* effect emanating from the strong  $\sigma$ -donating ability of the cyclometallating carbon affects the Ir–N<sub>pic</sub> bond lengths.<sup>39</sup> The latter are roughly of 2.13 Å for the three structures, much longer than the other Ir–N<sub>C<sup>^</sup>N</sub> lengths which are of the order of 2.04 Å. The bite angles of both cyclometallating ligand and ancillary ligand are similar through the series and comparable with [Ir(ppy)<sub>2</sub>pic]; the bite angles of ppy ligand and 2-phenylbenzimidazole are around 80°. The C–Ir–C' angles are about 90.5° for the three complexes of the same order of the one encountered in [Ir(ppy)<sub>2</sub>pic] (88.7°). Brought together, the different parameters are coherent with the expected octahedral coordination geometry, with slight distortions of the ligands caused by the formation of the five-membered metallacycles.<sup>39,69–72</sup> A particularity observed through the three complexes is the strong interaction between the hydrogen atoms from CH<sub>3</sub>CHCH<sub>3</sub> and the *ortho* H from the benzimidazole ring: these two atoms display a distance very inferior to 2.29 Å corresponding to the sum of the Van der Waals radii (VdW), ranging from 1.913 Å to 2.055 Å. These strong interactions have been observed before in a cationic series of iridium complexes,<sup>64</sup> and they could be the origin of the strong distortions observed in the cyclometallating ligand (~13°), larger than the ones observed in [Ir(ppy)<sub>2</sub>pic] (~4°). It is worth noting that these interactions are also observed in solution at room temperature, notably on the <sup>1</sup>H NMR spectrum, as the *iso*-propyl's methyl groups are not equivalent, even at higher temperature, and the central H is observed at lower field than the expected chemical shift (3–4.5

Figure 1: X-ray molecular structure of complexes **IrL<sup>6</sup><sub>2</sub>**, **IrL<sup>9</sup><sub>2</sub>** and **IrL<sup>10</sup><sub>2</sub>**. Thermal ellipsoids are plotted at the 50 % probability level. H atoms and solvent molecules are omitted for clarity.

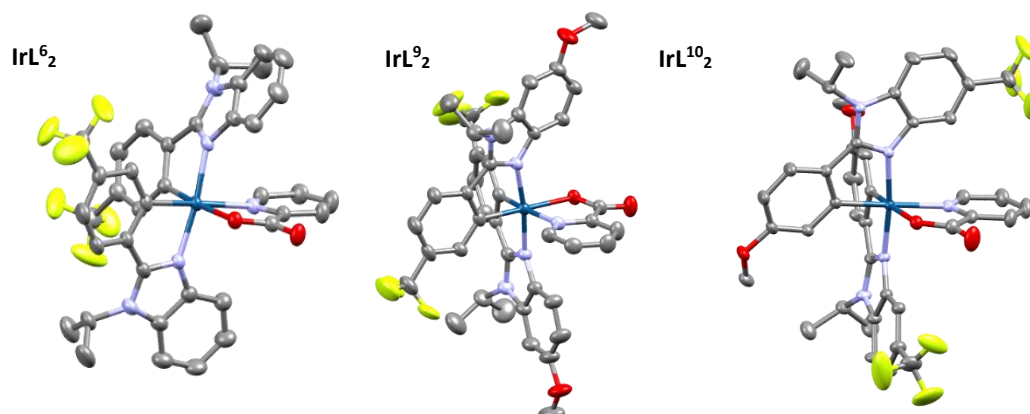


Table 1 Some relevant bonding and angles parameters for complexes **IrL<sup>6</sup>pic**, **IrL<sup>9</sup>pic** and **IrL<sup>10</sup>pic** along with **[Ir(ppy)<sub>2</sub>(pic)]<sup>65</sup>** for comparison purpose.

Complex	[Ir(ppy) <sub>2</sub> (pic)] <sup>65</sup>	IrL <sup>6</sup> <sub>2</sub>	IrL <sup>9</sup> <sub>2</sub>	IrL <sup>10</sup> <sub>2</sub>
Ir – C (Å)	2.003(6),	1.995(5),	2.003(5),	1.995(2),
	2.012(5)	2.020(5)	2.006(5)	2.009(2)
Ir – NC <sup>^</sup> N (Å)	2.041(5),	2.043(3),	2.031(3),	2.028(2),
	2.052 (5)	2.049(3)	2.037(3)	2.031(2)
		2.031(3),	2.037(3)	2.031(2)
		2.037(3)		
Ir – NN <sup>^</sup> O (Å)	2.141(5)	2.130(3)	2.121(3)	2.134(2)
Ir – ON <sup>^</sup> O (Å)	2.156(4)	2.147(3)	2.151(3)	2.157(2)
C – Ir – C' (°)	88.7(2)	90.5(2)	91.7(2)	89.37(8)
NC <sup>^</sup> N – Ir – NC <sup>^</sup> N (°)	175.7(2)	172.6(1)	172.5(1)	173.56(8)
CγC <sup>^</sup> N – Ir – ON <sup>^</sup> O (°)	95.4(2)	94.8(2)	93.5(2)	97.93(7)
CδC <sup>^</sup> N – Ir – NN <sup>^</sup> O (°)	100.1(2)	97.8(2)	97.8(2)	96.01(7)
N <sup>^</sup> O bite angle (°)	77.1(2)	76.9(1)	77.1(1)	76.81(6)
C <sup>^</sup> N bite angle (°)	80.1(2),	79.2(2),	79.6(2),	79.14(7),
	81.3(2)	79.6(2)	79.6(2)	79.62(7)
Distortion C <sup>^</sup> N (°)	2.60, 5.71	15.18,	12.34,	8.95,
		17.30	12.90	10.45
Distortion N <sup>^</sup> O (°)	4.54	6.74	3.60	4.40
H30-H19	-	2.055	2.048	1.943
H3-H14 (Å)	-	2.025	1.957	1.913

Distortion C<sup>^</sup>N are defined by the angle between the mean plans of the benzimidazole moiety and the phenyl and distortion N<sup>^</sup>O (picolato ligand) by the angle of the mean planes of the COO function and the corresponding pyridine.

Table 2: Redox potentials of complexes **IrL<sup>n</sup>pic** E(V) vs Ag/AgNO<sub>3</sub> (0.01 M) in deaerated CH<sub>3</sub>CN.

Complex	E <sub>red</sub> (V)	E <sub>ox</sub> (V)
IrL <sup>1</sup> <sub>2</sub>	-2.38	0.61
IrL <sup>2</sup> <sub>2</sub>	-2.20 <sup>irr</sup>	0.71
IrL <sup>3</sup> <sub>2</sub>	-2.38	0.57
IrL <sup>4</sup> <sub>2</sub>	-2.34	0.70
IrL <sup>5</sup> <sub>2</sub>	-2.38	0.60
IrL <sup>6</sup> <sub>2</sub>	-2.42 <sup>irr</sup>	0.84
IrL <sup>7</sup> <sub>2</sub>	-2.38	0.55
IrL <sup>8</sup> <sub>2</sub>	-2.21 <sup>irr</sup>	0.94
IrL <sup>9</sup> <sub>2</sub>	-2.41 <sup>irr</sup>	0.80
IrL <sup>10</sup> <sub>2</sub>	-2.34	0.71

<sup>irr</sup> denoted irreversible reduction peak

ppm) in all the complexes, with multiplets displayed between 5.8 ppm and 5.56 ppm.

One can notice that, the crystal packings of the three complexes display several hydrogen bonds between adjacent complexes, involving the oxygen atoms of the picolate ligand and with distances ranging from 2.397 to 2.679 Å that are inferior to the VdW sum ( $\Sigma_{\text{VdW}}(\text{H}_{\text{Ar}}-\text{O}) = 2.61$  Å and  $\Sigma_{\text{VdW}}(\text{H}_{\text{Al}}-\text{O})$

= 2.72 Å). Other hydrogen bonds are present involving fluorine atoms from the CF<sub>3</sub> group and H...π interactions are also present. These interactions are characterized considering the distances H-X that are inferior to the VdW sum ( $\Sigma_{\text{VdW}}(\text{H}_{\text{Ar}}-\text{C}_{\text{Ar}}) = 2.79$  Å,  $\Sigma_{\text{VdW}}(\text{H}_{\text{Ar}}-\text{F}) = 2.56$  Å,  $\Sigma_{\text{VdW}}(\text{H}_{\text{Al}}-\text{F}) = 2.67$  Å, and  $\Sigma_{\text{VdW}}(\text{H}_{\text{Al}}-\text{C}_{\text{Ar}}) = 2.90$  Å). The supramolecular bonds seem to be mainly driven by electrostatic interaction, to the exception of the upper mentioned interaction between H30 and H19 that is due to structural hindrance.<sup>73,74</sup>

From a computational point of view, the relaxed ground state structures are in very good agreement with respect to experiment. For instance, for complex **IrL<sup>6</sup><sub>2</sub>**, the averaged Ir-C and Ir-NC<sup>^</sup>N computed (experimental) values are 2.002 (2.019) and 2.051 (2.039) Å. Also, the Ir-NN<sup>^</sup>O and Ir-O-N<sup>^</sup>O are simulated at 2.150 and 2.171 Å matching nicely the observed ones using XRD (2.130 and 2.147 Å). These results gave us confidence for the rationalization of the ground and excited state optoelectronic properties.

**The electrochemical properties** of the complexes have been studied by cyclic voltammetry (CV) in deaerated 10<sup>-2</sup> M solution of *n*-NBu<sub>4</sub>PF<sub>6</sub> in MeCN as supporting electrolyte, using vitreous carbon working electrode (5 mm) and Ag/AgNO<sub>3</sub> (10<sup>-2</sup> M) as reference electrode at a scan rate of 100 mV s<sup>-1</sup>. The redox potentials are given *versus* the reference electrode. CV traces are shown in Figure S1, and values are gathered in Table 2. In agreement with previous work on similar complexes, the oxidation peaks in the range 0.55–0.94 V are ascribed to the Ir<sup>III</sup>/Ir<sup>IV</sup> couple, whereas the reduction affects principally the cyclometalating ligand.<sup>52,75</sup> Complex **IrL<sup>1</sup><sub>2</sub>** displays a E<sub>red</sub> at -2.38 V and a E<sub>ox</sub> at 0.61 V, whereas the parent complex [Ir(ppy)<sub>2</sub>(pic)] has a smaller  $\Delta E_{\text{redox}}$  with E<sub>red</sub> at -2.27 V and a E<sub>ox</sub> at 0.66 V.<sup>76</sup> The differences can be explained by the fact that 2-phenylbenzimidazole is more electron rich than 2-phenylpyridine, which leads **IrL<sup>1</sup><sub>2</sub>** to be more easily oxidized (i.e. the metal center easier to oxidize) and, consequently, more difficult to be reduced. As expected, the electrochemical properties of the complexes are sensitive to the nature of the substituents, both over the benzimidazole and the phenyl moieties. In reduction, most of the complexes display a reversible reduction wave, to the exception of four of the complexes, whose cyclometalating ligands are substituted by chlorine atoms (**IrL<sup>2</sup><sub>2</sub>**) and by CF<sub>3</sub> group on the phenyl ring (**IrL<sup>6,8,9,2</sup><sub>2</sub>**). The introduction of the electron withdrawing groups CF<sub>3</sub> on the benzimidazole moiety shifts the reduction to less negative potential (**IrL<sup>2</sup><sub>2</sub>**, E<sub>red</sub> = -2.20 V and **IrL<sup>4</sup><sub>2</sub>**, E<sub>red</sub> = -2.34 V) in comparison with **IrL<sup>1</sup><sub>2</sub>**. In contrast, the introduction of electron donating groups (OMe) solely, either on the benzimidazole and/or the phenyl moieties, does not induce a decrease of the reduction potential (**IrL<sup>3,5,7,2</sup><sub>2</sub>**, E<sub>red</sub> = -2.38 V) with respect to **IrL<sup>1</sup><sub>2</sub>**. In the case of the position isomers substituted both by CF<sub>3</sub> and by OMe groups on the cyclometalating ligand, the influence of the electrodonating group prevails on the reduction potential, albeit the reduction peaks of complexes **IrL<sup>6,9,8,2</sup><sub>2</sub>** are irreversible. Such a behaviour has been previously described.<sup>64</sup> In oxidation, all the complexes display a reversible peak whose potential is depending on the substituent. As expected, the electron

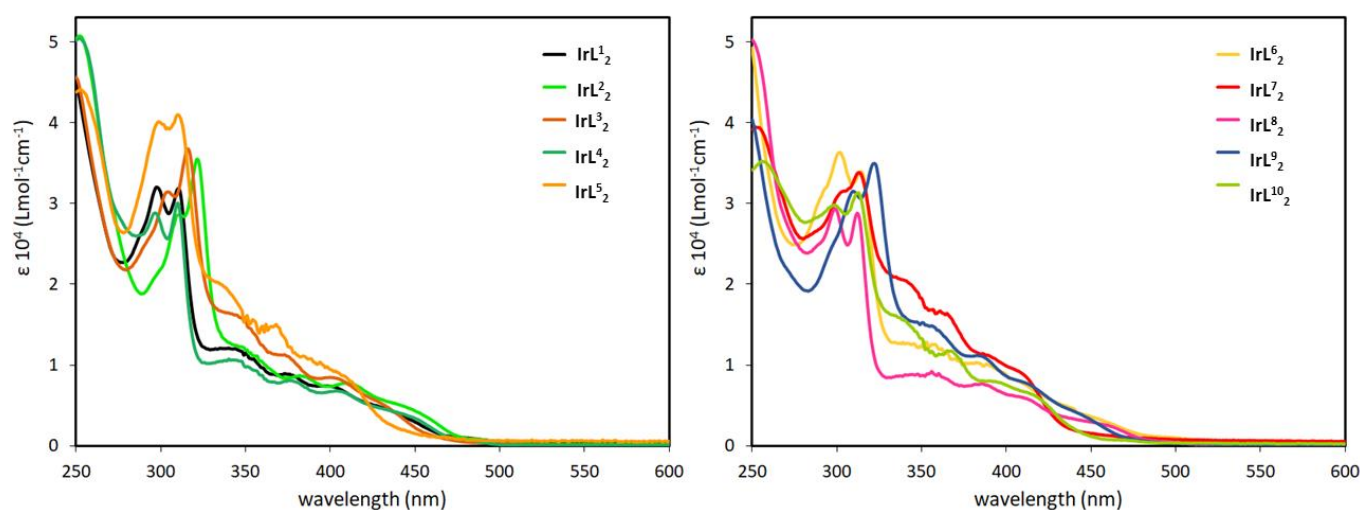


Figure 2: Absorption spectra of the ten complexes in  $\text{CH}_2\text{Cl}_2$  at room temperature.

withdrawing  $\text{CF}_3$  group and chlorine atoms lead to a more positive  $E_{\text{ox}}$  in comparison with  $\text{IrL}_2$ . The influence is greater when the group is on the phenyl rather than on the benzimidazole. This agrees with the fact that the HOMO is localized on the Ir-phenyl moiety.<sup>52,77,78</sup> Similarly, the electron donating OMe group, both on the benzimidazole and the phenyl, has for consequence to decrease  $E_{\text{ox}}$  (vs  $\text{IrL}_2$ ). However, one can notice that the substitution by  $\text{CF}_3$  groups on both “sides” of the cyclometallating ligand has a synergetic effect on  $E_{\text{ox}}$  ( $\text{IrL}_4$ ,  $E_{\text{ox}} = 0.70$  V; and  $\text{IrL}_8$ ,  $E_{\text{ox}} = 0.94$  V); the synergy is less effective in the case of OMe ( $\text{IrL}_3$ ,  $E_{\text{ox}} = 0.57$  V; and  $\text{IrL}_7$ ,  $E_{\text{ox}} = 0.55$  V) as the potentials with one or two MeO are almost identical. The presence of both OMe and  $\text{CF}_3$  groups on the cyclometallating ligand demonstrates the prevalence of the electron withdrawing group over the electron donating group, as shown by the  $E_{\text{ox}}$  0.80 V and 0.71 V of  $\text{IrL}_9$  and  $\text{IrL}_{10}$ , respectively. One should notice that the incorporation of two OMe moieties for the complex  $\text{IrL}_7$  induces a less positive oxidation potential than for other complexes. It should be also noticed that, as expected, all complexes possessing such donating group have a HOMO partly localized on the OMe moiety. The cyclometallating ligand 2-phenylbenzimidazole, used instead of the most

encountered 2-phenylpyridine (ppy), has a substantial effect on the electrochemical properties of complexes in comparison with  $[\text{Ir}(\text{ppy})_2\text{pic}]$ .

## Photophysical properties

**Absorption spectroscopy.** The absorption spectra of the complexes have been registered in dilute solution of  $\text{CH}_2\text{Cl}_2$  at room temperature, they are displayed in Figure 2 and data are gathered in Table 3 (individual absorption spectra are presented in fig S2). The intense bands around 300 nm can be ascribed to ligand-centred (LC)  $\pi\text{-}\pi^*$  transitions from the cyclometallating and ancillary ligands. Broad and relatively weak absorption bands observed in the longer wavelength region, over 350 nm, is the overlap of metal-to-ligand charge transfer (MLCT) and ligand-to-ligand charge transfer (LLCT) and over roughly 460 nm direct absorption from singlet ground state to triplet excited state (Figure S3), consequence of the strong spin orbit coupling effect exerted by the Ir(III) core.<sup>7,8,30,79,80</sup> For instance, the less intense lowest-lying bands, displayed as weak tails in the absorption spectra, roughly around 430 nm are ascribed to spin-forbidden triplet transitions. As expected, a focus on the CT absorption bands

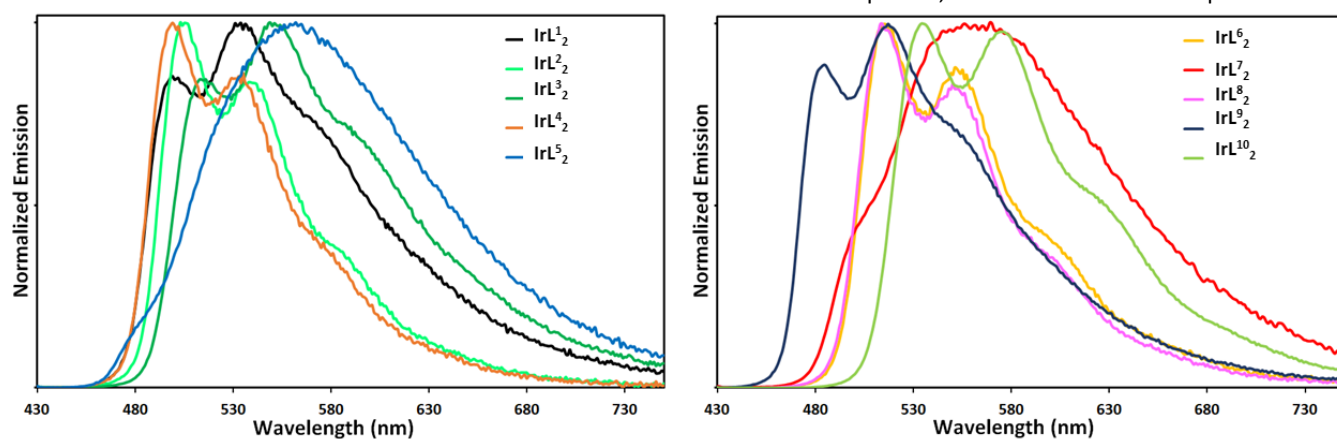


Figure 3: Emission spectra of the ten complexes in diluted solution of  $\text{CH}_2\text{Cl}_2$  at room temperature.



wavelength evidences the influence of the substituents: for instance, electron withdrawing groups ( $\text{CF}_3$  and  $\text{Cl}$ ) induce a hypsochromic shift and *a contrario* the electron donating methoxy group induces a bathochromic shift. It seems that the influence of the substituent on the absorption bands energies is not greatly depending on the position on the cyclometallating ligand. To assign the observed absorption bands, TD-DFT computations were conducted on the relaxed ground state geometries. The simulated spectra, along with the band assignments, have been compiled in the supplementary information (Table S 2 and Figure S 32). It should be noted that the simulated spectra match the experimental trend well.

The primary transition is a mixture of MLCT and LLCT (L= phenyl-benzimidazole) in all complexes except for  $\text{IrL}^6_2$  and  $\text{IrL}^8_2$ . Additionally, all complexes exhibit a weak initial transition (with a small oscillator strength) that corresponds to ML'CT and LL'CT (charge towards the picolate moieties), except for  $\text{IrL}^7_2$  and  $\text{IrL}^{10}_2$  which possess two rather strong transitions that are close in energy.  $\text{IrL}^5_2$  is the only complex that exhibits two very weak transitions corresponding to ML'CT and LL'CT before the primary transition (MLCT and LLCT). Moreover, this strong transition is approximately 0.20 eV higher in energy than in the other complexes. Complex  $\text{IrL}^7_2$  also exhibits such a pattern. These differences compared to other complexes may explain a distinct excited state energy order for these complexes.

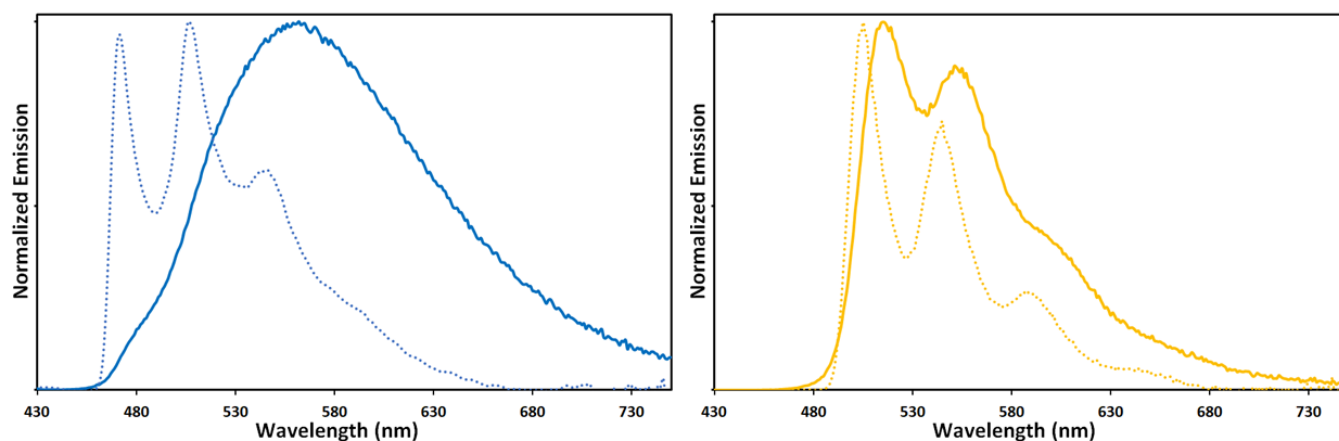
**Emission spectroscopy.** The emission spectra of the complexes have been recorded in both deaerated and air equilibrated dilute solution of  $\text{CH}_2\text{Cl}_2$  at room temperature and at 77 K in butyronitrile rigid matrix. The room temperature spectra are displayed in Figure 4, the photophysical data are gathered in Table 3 and the individual spectra are to be found in SI as well as those at 77 K. At r.t., the complexes display structured emission spectra (to the exception of  $\text{IrL}^5_2$  and  $\text{IrL}^7_2$  whose emission spectra are broad) in the visible range, with lifetimes of  $\mu\text{s}$ , with large Stokes shifts, and sensitivity to the presence of oxygen ( $k[\text{O}_2]$  ranging from  $1.8 \text{ M}^{-1} \text{ s}^{-1}$  to  $5.5 \text{ M}^{-1} \text{ s}^{-1}$

1). Therefore the emission can be ascribed to phosphorescence as expected for this family of iridium(III) complexes. The photoluminescence quantum yields are ranging from 0.04 to 0.43 in deaerated  $\text{CH}_2\text{Cl}_2$ . The photophysical properties of  $(\text{ppy})_2\text{Irpic}^{81}$  are worth to compare with  $\text{IrL}^1_2$ .  $(\text{ppy})_2\text{Irpic}$  displays an emission at 505 nm ( $\phi = 0.15$ ,  $\tau = 514 \text{ ns}$ , deaerated) in  $\text{CH}_2\text{Cl}_2$  which is comparable with  $\text{IrL}^1_2$ , but the use of 2-phenylbenzimidazole instead of 2-phenylpyridine as cyclometallating ligand seems to induce a broadening of the emission band with a concomitant more pronounced vibronic progression.<sup>81</sup> Albeit, in both complexes the nature of the emitting excited state is predominantly  $^3\text{IL}$ , in view of the slight rigidochromism ( $\sim 10 \text{ nm}$ ) observed at low temperature.

The introduction of electron withdrawing group solely (i.e.  $\text{CF}_3$  and  $\text{Cl}$ ) either on the benzimidazole ( $\text{IrL}^2_2$  and  $\text{IrL}^4_2$ ) or on the cyclometallating cycle ( $\text{IrL}^6_2$ ) does not induce pronounced hypsochromic shift in comparison with  $\text{IrL}^1_2$ . As a consequence,  $\text{IrL}^4_2$  and  $\text{IrL}^2_2$  display emission spectra in the same range as  $\text{IrL}^1_2$ , whereas  $\text{IrL}^6_2$  displayed a slight bathochromic shift ( $E^{00} = 2.20 \text{ eV}$ ). Along these four complexes the shape of the spectra changes by getting more structured, which is accompanied by an increase of the  $k_r$  (i.e. radiative rate constant) from  $2.8 \cdot 10^5 \text{ s}^{-1}$  to  $3.9 \cdot 10^5 \text{ s}^{-1}$ , for  $\text{IrL}^1_2$  and  $\text{IrL}^6_2$  respectively. On the other hand, the introduction of electron donating group solely on either the benzimidazole ( $\text{IrL}^3_2$ ) or the cyclometallating ring ( $\text{IrL}^5_2$ ) induces a slight bathochromic shift in comparison with  $\text{IrL}^1_2$ , with  $E^{00}$  of 2.47 eV, 2.40 eV and 2.20 eV for  $\text{IrL}^1_2$ ,  $\text{IrL}^3_2$ , and  $\text{IrL}^5_2$  respectively. The  $k_r$  is  $1.2 \cdot 10^5 \text{ s}^{-1}$  for both  $\text{IrL}^3_2$  and  $\text{IrL}^5_2$ , smaller than the  $k_r$  ( $2.8 \cdot 10^5 \text{ s}^{-1}$ ) observed for  $\text{IrL}^1_2$  and, in addition,  $\text{IrL}^5_2$  displays a broad emission.

The substitution by electron withdrawing ( $\text{IrL}^8_2$ ) or by electron donating ( $\text{IrL}^7_2$ ) groups on both "sides" of the 2-phenylbenzimidazole does induce slight changes in the emission energy. The presence of two  $\text{CF}_3$  groups in  $\text{IrL}^8_2$  draws a hypsochromic shift of the emission (in accordance with the  $E^{00}$  of 2.40 eV) and the radiative rate constant decreases

Figure 4: Superimposition of the emission spectra at room temperature (full line) in  $\text{CH}_2\text{Cl}_2$  and at 77 K (dashed line) in butyronitrile of complexes  $\text{IrL}^5_2$  (left) and  $\text{IrL}^8_2$  (right).



slightly ( $2.2 \times 10^5 \text{ s}^{-1}$ ), in comparison with  $\text{IrL}^1_2$ . On the other hand, the similar substitution by MeO groups for  $\text{IrL}^7_2$  has quite a dramatic consequence on the emission spectrum shape, which becomes structureless and displays a bathochromic shift with an  $E^{00}$  of 2.21 eV. One can notice that the  $k_r$  are similar for these two complexes,  $2.8 \times 10^5 \text{ s}^{-1}$ . Finally, the last two position isomers  $\text{IrL}^9_2$  and  $\text{IrL}^{10}_2$  substituted by antagonist functional groups in different position,  $\text{CF}_3$  and OMe, exhibit distinct emission spectra. Both spectra are structured with similar radiative constants,  $2.2 \times 10^5 \text{ s}^{-1}$  and  $2.6 \times 10^5 \text{ s}^{-1}$ , respectively for  $\text{IrL}^9_2$  and  $\text{IrL}^{10}_2$ , that are below the one observed for  $\text{IrL}^1_2$  ( $k_r = 2.8 \times 10^5 \text{ s}^{-1}$ ), particularly for  $\text{IrL}^9_2$ . The impact of the position of the substituent is dramatic when looking at the emission energy, while  $\text{IrL}^9_2$  displays a hypsochromic shift, with  $E^{00}$  of 2.56 eV,  $\text{IrL}^{10}_2$  spectrum is red shifted, with  $E^{00}$  of 2.31 eV, both with respect to  $\text{IrL}^1_2$  (2.47 eV). The  $^3\text{MLCT}$  or  $^3\text{LC}$  nature of the phosphorescence emitting excited states can be experimentally assessed by the photophysical properties.<sup>11,42</sup> For instance, a typical  $^3\text{MLCT}$  emission like that of *fac*-Ir(ppy)<sub>3</sub> will display a radiative constant around  $2 \times 10^5 \text{ s}^{-1}$  ( $\tau \sim 2 \mu\text{s}$ ), and for the case of a pure  $^3\text{LC}$  emission the radiative constant will be smaller, like that of (thpy)<sub>2</sub>Ir(acac)<sup>82</sup> (thpy = 2-(2-pyridyl)benzothiophene; acac = acetylacetonate) which displays a  $kr$  of  $0.2 \times 10^5 \text{ s}^{-1}$  ( $\tau \sim 5.3 \mu\text{s}$ ). Within the series, the radiative constants are ranging from  $1.2 \times 10^5 \text{ s}^{-1}$  to  $3.9 \times 10^5 \text{ s}^{-1}$ , which seems to indicate that most of the complexes display an emission emanating from the radiative deactivation of a lowest  $^3\text{MLCT}$  state, to the exception of  $\text{IrL}^3_2$  and  $\text{IrL}^5_2$ , whose radiative constant are significantly lower than  $2 \times 10^5 \text{ s}^{-1}$ . However,  $kr$  is not the only parameter that allows to characterize the nature of the lowest excited state and other experimental parameters have to be considered: (i) the shape of the emission spectrum which is structureless and broad for an emission emanating from a  $^3\text{MLCT}$ , (ii) the rigidochromic effect at low temperature, and (iii) the linear relationship<sup>83</sup> for  $^3\text{MLCT}$  emission between the emission energy and  $\Delta E_{1/2} = (E_{\text{ox}} - E_{\text{red}})$  eV. Thus, with regard to the shape of the spectrum, only  $\text{IrL}^5_2$  and  $\text{IrL}^7_2$  display a broad and structureless emission which is characteristic of a  $^3\text{MLCT}$  emission. The rigidochromism is a property of the transition metal complexes with an emission emanating from the radiative deactivation of  $^3\text{CT}$  excited state, typically  $^3\text{MLCT}$ , displaying a blue shifted emission when their solution environment becomes rigid, by lowering temperature in solution.<sup>38</sup> The superimposed spectra at r.t. and in benzonitrile at 77 K are presented in Figure S4. Looking at the spectra, two pictures are observed, being a marked rigidochromism and a slight one.



Table 3: Photophysical Properties

Complex	absorption $\lambda$ [nm] ( $\epsilon \times 10^3$ [M <sup>-1</sup> cm <sup>-1</sup> ])	Photoluminescence in dilute solution of CH <sub>2</sub> Cl <sub>2</sub> , 298 K <sup>a,b</sup>							Photoluminescence at 77 K <sup>c</sup>	
		$\lambda$ [nm]	$\Phi$ (air)	$\tau$ [ $\mu$ s] (air)	$k_r \times 10^5$ [s <sup>-1</sup> ]	$k_{nr} \times 10^5$ [s <sup>-1</sup> ]	$k[O_2]^d \times 10^9$ [M <sup>-1</sup> s <sup>-1</sup> ]	$E^{00e}$ (eV)	$\lambda$ /nm	$\tau$ ( $\mu$ s)
IrL <sup>1</sup> <sub>2</sub>	298 (31.9), 310 (31.8), 345 (11.9), 375 (8.8), 402 (7.3), 429 (4.8), 480 (1.0)	503, 537*	0.09 (0.02)	0.32 (0.08)	2.8	28.4	5.0	2.47	486*, 521, 567	3.31
IrL <sup>2</sup> <sub>2</sub>	309 (28.3), 322 (35.4), 350 (11.8), 382 (8.2), 413 (7.7), 441 (5.1), 488 (0.8)	507*, 542, 587sh	0.35 (0.03)	1.10 (0.12)	3.5	5.9	4.4	2.45	490*, 530, 573, 627sh	2.94
IrL <sup>3</sup> <sub>2</sub>	304 (31.4), 316 (36.7), 347 (15.8), 374 (11.1), 403 (8.4), 431 (5.1), 493 (0.3)	516, 552*, 600sh	0.11 (0.01)	0.89 (0.10)	1.2	10.0	5.1	2.40	500*, 537, 584, 640sh	4.10
IrL <sup>4</sup> <sub>2</sub>	297 (28.8), 309 (29.7), 343 (10.7), 376 (8.4), 408 (6.7), 442 (3.5), 484 (0.7)	502*, 532, 580sh	0.42 (0.03)	1.21 (0.12)	3.5	4.8	4.9	2.47	488*, 521, 563, 616sh	3.49
IrL <sup>5</sup> <sub>2</sub>	299 (40.1), 311 (40.8), 336 (20.0), 369 (14.7), 410 (8.4), 468 (1.1)	563	0.04 (0.01)	0.32 (0.08)	1.2	30.0	4.3	2.20	471, 507*, 547	4.58
IrL <sup>6</sup> <sub>2</sub>	302 (36.3), 314 (33.9), 357 (12.5), 387 (9.9), 408 (7.7), 449 (3.7), 496 (1.0)	514*, 554, 605sh	0.40 (0.03)	1.02 (0.19)	3.9	5.9	5.5	2.41	505*, 544, 589	4.40
IrL <sup>7</sup> <sub>2</sub>	302 (30.8), 313 (33.3), 341 (19.9), 362 (15.9), 389 (10.7), 410 (8.4), 457 (0.8)	500sh, 560*	0.30 (0.04)	1.07 (0.19)	2.8	6.5	2.8	2.48	486*, 526, 569, 621sh	6.75
IrL <sup>8</sup> <sub>2</sub>	298 (29.4), 312 (28.7), 358 (8.8), 387 (7.6), 412 (5.8), 462 (2.3), 491 (0.6)	516*, 554, 600sh	0.43 (0.05)	1.91 (0.23)	2.2	3.0	1.8	2.40	500*, 541, 584	4.31
IrL <sup>9</sup> <sub>2</sub>	309 (31.9), 322 (35.0), 356 (14.9), 384 (11.2), 412 (7.8), 446 (3.7), 491 (0.4)	485, 519*, 554sh	0.17 (0.02)	0.78 (0.10)	2.2	10.6	4.4	2.56	470*, 506, 544	3.35
IrL <sup>10</sup> <sub>2</sub>	299 (29.7), 313 (30.8), 337 (15.8), 367 (11.7), 395 (7.9), 416 (6.3), 472 (0.6)	536*, 578, 627sh	0.24 (0.03)	0.91 (0.08)	2.6	8.3	3.5	2.31	519*, 562, 612	4.04

<sup>a</sup> Ir(ppy)<sub>3</sub> in CH<sub>2</sub>Cl<sub>2</sub> was used as a reference. <sup>b</sup> In deaerated solution unless otherwise mentioned. <sup>c</sup> Recorded in butyronitrile. <sup>d</sup> With [O<sub>2</sub>] = 2.2 mM in dichloromethane. <sup>e</sup> Energy of the emitting excited state. \*The most intense band

Table 4: Selected photophysical parameters

Complexes  $\text{IrL}^5_2$  and  $\text{IrL}^6_2$  are very representative and the superimposed spectra are shown in Figure 4. It is somewhat striking that the emission spectra at r.t. in  $\text{CH}_2\text{Cl}_2$  and at 77 K in butyronitrile are almost superimposed for  $\text{IrL}^6_2$ . Within the series, only  $\text{IrL}^5_2$  and  $\text{IrL}^7_2$  exhibit broad emission spectra at r.t., displaying a strong rigidochromic effect and a change in the spectra shape. Finally, the linear relation between the emission energy and  $\Delta E_{1/2}$  is not verified within the series, which rules out an emission emanating from the pure  $^3\text{MLCT}$  for this family of complexes. To conclude, while the excited states ( $^3\text{IL}$ ,  $^3\text{ILCT}$  and  $^3\text{MLCT}$ ) are known to be very close in iridium(III) complexes, it seems that, at the light of the experimental results, the present series of complexes displays an emission at r.t. with a strong proportion of  $^3\text{IL}$  excited state, to the exception of  $\text{IrL}^5_2$  and  $\text{IrL}^7_2$ , whose emission at r.t. have strong  $^3\text{MLCT}$  character. As the primary transition is a mixture of MLCT and LLCT (see above), the complexes rapidly undergo intersystem crossing and the  $^3\text{MLCT}$  and  $^3\text{ILCT}$  are populated and a subsequent internal conversion leads to the population of the  $^3\text{IL}$  excited state.

To gain a deeper understanding of the phosphorescence properties, we performed optimizations of the first triplet excited state and simulations of the luminescence resulting from this state. As shown in Figure S33 of the supplementary information, our simulated spectra match the recorded spectra at room temperature. The relative intensities and peak positions are well-reproduced in our simulations, and we accurately replicate the spacing between the peaks in cases where there is sufficient vibronic coupling. Additionally, our simulations capture the bell-curve shape observed in the luminescence spectra of  $\text{IrL}^5_2$  and  $\text{IrL}^7_2$ , further validating our model. The correlation between the simulated and observed luminescence at room temperature is shown in Figure S34. This high level of agreement allows us to confidently localize the electrons in the excited state (spin density) and estimate the expected colour using a CIE (x,y) horseshoe diagram. Most of the complexes have a spin density localized over the metal and phenyl-benzimidazole moieties (Figure S35). However, for  $\text{IrL}^5_2$  and, surprisingly,  $\text{IrL}^9_2$ , the spin density is localized on the metal and the picolinate moieties, with a larger spin density on the picolinate for  $\text{IrL}^5_2$  than for  $\text{IrL}^9_2$ . These findings explain the distinctive behaviour of complex  $\text{IrL}^5_2$  compared to the others. Finally, we can compare the predicted colours from our simulations with the observed ones, as shown in Figure 5. As one can see, our simulations reproduce nicely the observed colour.

## Conclusion

We described a series of ten original 2-phenylbenzimidazole-based iridium(III) complexes with picolinate ancillary ligand, which have been characterized by NMR, HRMS and elemental analysis. Their luminescence properties have been studied in dilute solution at room temperature and in butyronitrile at low temperature, both in steady state and in time resolved

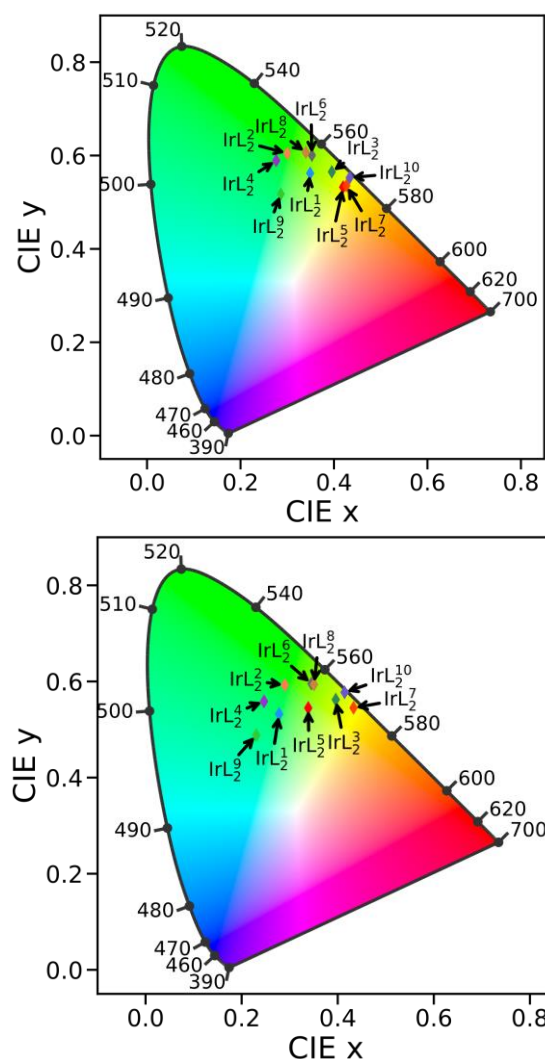


Figure 5 Chromaticity diagram CIE-1931: experimental (top) and simulated (bottom) color.

spectroscopy. We demonstrated that the choice of the substituent on the cyclometallating ligand allows to finely tune the emission energy of the complexes by playing on the electronic properties (i.e. Hammett parameter), which also has an influence on the electrochemical properties. Moreover, the nature of the lowest-lying excited state(s) is affected by the substituents and their position, and the emission emanates from the radiative deactivation of  $^3\text{CT}$  or  $^3\text{IL}$  excited states, in particular  $\text{IrL}^5_2$  can be recognized as a “genuine”  $^3\text{MLCT}$  emitter whereas  $\text{IrL}^6_2$  displays the opposite behaviour being a “true”  $^3\text{IL}$  emitter, which has been demonstrated by both experimental techniques and state-of-the-art computational methods.

## Experimental

### Synthesis of the complexes

The crude  $\mu$ -dichlorodimers were synthesized from  $\text{HL}^1$  –  $\text{HL}^{10}$  and  $\text{IrCl}_3 \cdot n\text{H}_2\text{O}$  as reported in our previous work.<sup>64</sup> In a round

bottom flask under argon, the selected  $\mu$ -dichloridodimer, 2-picolinic acid and  $\text{Na}_2\text{CO}_3$  (1:3:3) were dissolved in a deaerated 3:1 mixture of 2-ethoxyethanol/water and heated at 100 °C overnight. At r.t., water was added, and the precipitate was filtered off, washed with water, diethylether and dried. The precipitates were purified over pre-treated  $\text{SiO}_2$  with  $\text{Et}_3\text{N}$  using  $\text{CH}_2\text{Cl}_2/\text{CH}_3\text{OH}$  as eluent.

**IrL<sup>1</sup><sub>2</sub>**; Crude  $[\text{Ir}(\text{L}^1)_2(\mu\text{-Cl})_2]$  (0.041 g 0.06 mmol), 2-picolinic acid (0.022 g 0.18 mmol),  $\text{Na}_2\text{CO}_3$  (0.19 g 0.18 mmol) and 2-ethoxyethanol/water 3:1 (10 mL).  $\text{SiO}_2$  ( $\text{CH}_2\text{Cl}_2/\text{CH}_3\text{OH}$  9:1). Product isolated as yellow powder (41 mg 89%). <sup>1</sup>H NMR (500 MHz,  $\text{CD}_2\text{Cl}_2$ )  $\delta$  8.15 – 8.11 (m, 1H;  $\text{H}_\alpha$ ), 7.99 (dd,  $J$  = 8.0, 0.6 Hz, 1H;  $\text{H}_{10}$ ), 7.88 – 7.86 (m, 2H;  $\text{H}_\beta$ ,  $\delta$ ), 7.79 (d,  $J$  = 9.0 Hz, 1H;  $\text{H}_5$ ), 7.77 (d,  $J$  = 9.1 Hz, 1H;  $\text{H}_5$ ), 7.70 (d,  $J$  = 8.4 Hz, 1H;  $\text{H}_{13}$ ), 7.68 (d,  $J$  = 7.9 Hz, 1H;  $\text{H}_{13}$ ), 7.32 (td,  $J$  = 7.0, 1.5 Hz, 1H;  $\text{H}_\gamma$ ), 7.31 – 7.27 (m, 1H,  $\text{H}_{12}$ ), 7.27 – 7.23 (m, 1H;  $\text{H}_{11}$ ), 7.21 (ddd,  $J$  = 8.3, 7.3, 1.0 Hz, 1H,  $\text{H}_{12}$ ), 6.96 (dt,  $J$  = 15.2, 7.6 Hz, 2H,  $\text{H}_\alpha$ ,  $\delta$ ), 6.86 (ddd,  $J$  = 8.2, 7.4, 0.9 Hz, 1H;  $\text{H}_{11}$ ), 6.70 (tdd,  $J$  = 7.5, 3.4, 1.2 Hz, 2H;  $\text{H}_3$ ,  $\delta$ ), 6.51 (dd,  $J$  = 7.7, 0.9 Hz, 1H;  $\text{H}_2$ ), 6.22 (dd,  $J$  = 7.7, 0.9 Hz, 1H;  $\text{H}_2$ ), 5.80 – 5.67 (m, 3H;  $\text{H}_{10}$ ,  $2(\text{CH}(\text{CH}_3)_2)$ ), 1.86 (ddd,  $J$  = 9.8, 6.9, 4.9 Hz, 12H;  $2(\text{CH}(\text{CH}_3)_2)$ ). <sup>13</sup>C NMR (126 MHz,  $\text{CD}_2\text{Cl}_2$ )  $\delta$  173.4, 164.1, 163.1, 154.0, 152.6, 150.5, 149.8, 141.3, 141.2, 137.8, 136.0, 135.54, 135.46, 134.7, 134.2, 133.9, 129.9, 129.6, 128.1, 127.8, 125.7, 125.4, 124.3, 123.7, 123.1, 122.6, 121.7, 121.1, 117.9, 115.2, 114.3, 113.7, 50.3, 50.3, 22.1, 22.1, 21.9, 21.8. HRMS (ESI) found  $m/z$  786.24064 calcd  $m/z$  786.24166 for  $\text{C}_{38}\text{H}_{35}\text{IrN}_5\text{O}_2$  [M-H]<sup>+</sup>. Elemental Analysis calcd (%) for  $\text{C}_{38}\text{H}_{34}\text{IrN}_5\text{O}_2\cdot\text{CH}_3\text{OH}$ , C, 57.34; H, 4.69; N, 8.57, found C, 57.09; H, 4.74; N, 8.51.

**IrL<sup>2</sup><sub>2</sub>**; Crude  $[\text{Ir}(\text{L}^2)_2(\mu\text{-Cl})_2]$  (0.050 g 0.06 mmol), 2-picolinic acid (0.022 g 0.18 mmol),  $\text{Na}_2\text{CO}_3$  (0.019 g 0.18 mmol) and 2-ethoxyethanol/water 3:1 (10 mL). Purification over  $\text{SiO}_2$  was not possible due to the low solubility of the complex. The complex was washed with  $\text{H}_2\text{O}$ , diethylether and methanol, then recrystallized in a  $\text{CH}_2\text{Cl}_2$  /pentane mixture. The product was isolated as a pale-yellow powder (52 mg 95%). <sup>1</sup>H NMR (500 MHz,  $\text{CD}_2\text{Cl}_2$ )  $\delta$  8.19 (dd,  $J$  = 7.8, 0.5 Hz, 1H;  $\text{H}_\alpha$ ), 8.14 (s, 1H;  $\text{H}_{10}$ ), 7.95 (td,  $J$  = 7.7, 1.6 Hz, 1H;  $\text{H}_\beta$ ), 7.85 – 7.82 (m, 1H;  $\text{H}_\delta$ ), 7.80 – 7.78 (m, 3H,  $\text{H}_{13, 13'}$ ,  $\text{H}_5$ ), 7.77 (d,  $J$  = 7.9 Hz, 1H,  $\text{H}_5$ ), 7.40 (ddd,  $J$  = 7.5, 5.4, 1.5 Hz, 1H;  $\text{H}_\gamma$ ), 7.03 – 6.946 (m, 2H;  $\text{H}_\alpha$ ,  $\delta$ ), 6.78 – 6.72 (m, 2H;  $\text{H}_3$ ,  $\delta$ ), 6.51 (dd,  $J$  = 7.7, 0.8 Hz, 1H;  $\text{H}_2$ ), 6.20 (dd,  $J$  = 7.7, 0.8 Hz, 1H;  $\text{H}_2$ ), 5.69 (dh,  $J$  = 14.1, 6.9 Hz, 2H;  $2(\text{CH}(\text{CH}_3)_2)$ ), 5.58 (s, 1H,  $\text{H}_{10}$ ), 1.87 – 1.78 (m, 12H,  $2(\text{CH}(\text{CH}_3)_2)$ ). <sup>13</sup>C NMR (126 MHz,  $\text{CD}_2\text{Cl}_2$ )  $\delta$  173.2, 166.3, 165.2, 153.9, 152.7, 150.9, 149.9, 140.6, 140.4, 138.4, 135.6, 135.5, 134.7, 134.6, 133.4, 133.1, 130.7, 130.3, 128.6, 128.3, 128.2, 127.9, 127.1, 126.4, 126.2, 125.9, 122.1, 121.5, 118.8, 116.3, 115.3, 115.0, 54.0, 50.8, 50.8, 22.1, 22.0, 21.9, 21.8. HRMS (ESI) found  $m/z$  922.08386 calcd  $m/z$  922.08545 for  $\text{C}_{38}\text{H}_{31}\text{Cl}_4\text{IrN}_5\text{O}_2$  [M-H]<sup>+</sup>. Elemental Analysis calcd (%) for  $\text{C}_{38}\text{H}_{30}\text{Cl}_4\text{IrN}_5\text{O}_2$ , C, 49.46; H, 3.28; N, 7.59, found C, 49.54; H, 3.51; N, 7.62.

**IrL<sup>3</sup><sub>2</sub>**; Crude  $[\text{Ir}(\text{L}^3)_2(\mu\text{-Cl})_2]$  (0.054 g 0.06 mmol), 2-picolinic acid (0.024 g 0.19 mmol),  $\text{Na}_2\text{CO}_3$  (0.020 g 0.19 mmol) and 2-ethoxyethanol/water 3:1 (10 mL).  $\text{SiO}_2$  ( $\text{CH}_2\text{Cl}_2/\text{CH}_3\text{OH}$ ) progressive increase of  $\text{CH}_3\text{OH}$  from 1% to 6.5%. Product isolated as a yellow powder (46 mg 78%). <sup>1</sup>H NMR (500 MHz,  $\text{CD}_2\text{Cl}_2$ )  $\delta$  8.39 (s, 1H;  $\text{H}_{10}$ ), 8.17 (d,  $J$  = 7.7 Hz, 1H;  $\text{H}_\alpha$ ), 7.95 – 7.87

(m, 2H;  $\text{H}_\beta$ ,  $\delta$ ) 7.87 – 7.75 (m, 4H;  $\text{H}_{13, 13'}$ ,  $\text{H}_5$ ), 7.54 (d,  $J$  = 8.4 Hz, 1H;  $\text{H}_{12}$ ), 7.45 (d,  $J$  = 8.6 Hz, 1H;  $\text{H}_{12}$ ), 7.41 – 7.35 (m, 1H;  $\text{H}_\gamma$ ), 7.05 – 6.95 (m, 2H;  $\text{H}_\alpha$ ,  $\delta$ ), 6.75 (dd,  $J$  = 14.0, 6.9 Hz, 2H;  $\text{H}_3$ ,  $\delta$ ), 6.55 (d,  $J$  = 7.6 Hz, 1H;  $\text{H}_2$ ), 6.23 (d,  $J$  = 7.6 Hz, 1H;  $\text{H}_2$ ), 5.82 (s, 1H;  $\text{H}_{10}$ ) 5.81 – 5.71 (m, 2H;  $2(\text{CH}(\text{CH}_3)_2)$ ), 2.02 – 1.73 (m,  $J$  = 6.6 Hz, 12H;  $2(\text{CH}(\text{CH}_3)_2)$ ). <sup>13</sup>C NMR (126 MHz,  $\text{CD}_2\text{Cl}_2$ )  $\delta$  173.1, 166.4, 165.3, 154.0, 152.9, 151.2, 149.9, 140.9, 140.6, 138.3, 136.2, 136.0, 135.7, 135.2, 134.7, 130.7, 130.3, 128.24, 128.19, 128.16, 126.6, 126.4, 126.3, 126.12, 126.07, 126.0, 126.0, 125.8, 125.7, 123.9, 123.7, 122.0, 121.5, 120.00, 119.97, 119.9, 119.5, 119.4, 119.4, 115.52, 115.49, 115.45, 115.42, 114.7, 114.3, 112.71, 112.68, 112.64, 112.60, 50.81, 50.77, 22.15, 22.07, 22.0, 21.9. <sup>19</sup>F NMR (470 MHz,  $\text{CD}_2\text{Cl}_2$ )  $\delta$  -61.2, -61.5. HRMS (ESI) found  $m/z$  922.21578 calcd  $m/z$  922.21645 for  $\text{C}_{40}\text{H}_{33}\text{F}_6\text{IrN}_5\text{O}_2$  [M]<sup>+</sup>. Elemental Analysis calcd (%) for  $\text{C}_{40}\text{H}_{32}\text{F}_6\text{IrN}_5\text{O}_2$ , C, 52.16; H, 3.51; N, 7.61, found C, 51.92; H, 3.65; N, 7.75.

**IrL<sup>4</sup><sub>2</sub>**; Crude  $[\text{Ir}(\text{L}^4)_2(\mu\text{-Cl})_2]$  (0.067 g 0.09 mmol), 2-picolinic acid (0.032 g 0.27 mmol),  $\text{Na}_2\text{CO}_3$  (0.028 g 0.27 mmol) and 2-ethoxyethanol/water 3:1 (10 mL).  $\text{SiO}_2$  ( $\text{CH}_2\text{Cl}_2/\text{CH}_3\text{OH}$ ) progressive increase of  $\text{CH}_3\text{OH}$  until 5%. Product isolated as a yellow-orange powder (57 mg 76%). <sup>1</sup>H NMR (500 MHz,  $\text{CD}_2\text{Cl}_2$ )  $\delta$  8.15 – 8.11 (m, 1H;  $\text{H}_\alpha$ ), 7.90 – 7.83 (m, 3H;  $\text{H}_{10}$ ,  $\text{H}_\beta$ ,  $\delta$ ), 7.73 (d,  $J$  = 8.1 Hz, 1H;  $\text{H}_5$ ), 7.71 (d,  $J$  = 8.1 Hz, 1H;  $\text{H}_5$ ), 7.32 (dd,  $J$  = 5.6, 1.6 Hz, 1H,  $\text{H}_\gamma$ ), 7.15 (d,  $J$  = 2.3 Hz, 1H;  $\text{H}_{13}$ ), 7.12 (d,  $J$  = 2.2 Hz, 1H,  $\text{H}_{13}$ ), 6.98 – 6.88 (m, 3H;  $\text{H}_{11}$ ,  $\text{H}_\alpha$ ,  $\delta$ ), 6.71 – 6.65 (m, 2H;  $\text{H}_3$ ,  $\delta$ ), 6.50 (dd,  $J$  = 9.0, 2.4 Hz, 1H;  $\text{H}_{11}$ ), 6.48 (dd,  $J$  = 7.7, 1.0 Hz, 1H;  $\text{H}_2$ ), 6.21 (dd,  $J$  = 7.7, 0.9 Hz, 1H;  $\text{H}_2$ ), 5.69 (pd,  $J$  = 13.2, 6.3 Hz, 2H;  $2(\text{CH}(\text{CH}_3)_2)$ ), 5.56 (d,  $J$  = 9.0 Hz, 1H;  $\text{H}_{10}$ ), 3.86 (s, 3H; -OCH<sub>3</sub>), 3.83 (s, 3H; -OCH<sub>3</sub>), 1.88 – 1.79 (m, 12H;  $2(\text{CH}(\text{CH}_3)_2)$ ). <sup>13</sup>C NMR (126 MHz,  $\text{CD}_2\text{Cl}_2$ )  $\delta$  173.35, 163.58, 162.46, 156.79, 156.33, 154.00, 152.02, 149.79, 137.76, 136.33, 135.89, 135.77, 135.72, 135.28, 134.88, 134.62, 129.51, 129.19, 128.00, 127.73, 125.18, 124.95, 121.57, 120.98, 118.38, 115.68, 112.60, 112.19, 98.50, 98.19, 56.51, 56.48, 50.07, 21.85, 21.84, 21.72, 21.63. HRMS (ESI) found  $m/z$  846.26208 calcd  $m/z$  846.26281 for  $\text{C}_{40}\text{H}_{39}\text{IrN}_5\text{O}_4$  [M-H]<sup>+</sup>. Elemental Analysis calcd (%) for  $\text{C}_{40}\text{H}_{38}\text{IrN}_5\text{O}_4\cdot\text{H}_2\text{O}$ , C, 55.67; H, 4.67; N, 8.12, found C, 55.81; H, 4.75; N 7.98.

**IrL<sup>5</sup><sub>2</sub>**; Crude  $[\text{Ir}(\text{L}^5)_2(\mu\text{-Cl})_2]$  (0.049 g 0.06 mmol), 2-picolinic acid (0.022 g 0.18 mmol),  $\text{Na}_2\text{CO}_3$  (0.019 g 0.18 mmol) and 2-ethoxyethanol/water 3:1 (10 mL).  $\text{SiO}_2$  ( $\text{CH}_2\text{Cl}_2/\text{CH}_3\text{OH}/\text{Et}_3\text{N}$ ) progressive increase of  $\text{CH}_3\text{OH}$  from 1% to 6.5%. Product isolated as a bright yellow powder (29 mg 54%). <sup>1</sup>H NMR (500 MHz,  $\text{CD}_2\text{Cl}_2$ )  $\delta$  8.17 (dd,  $J$  = 7.8, 0.5 Hz, 1H;  $\text{H}_\alpha$ ), 8.02 (d,  $J$  = 8.0 Hz, 1H;  $\text{H}_{10}$ ), 7.91 (td,  $J$  = 7.7, 1.5 Hz, 1H;  $\text{H}_\beta$ ), 7.88 – 7.78 (m, 3H;  $\text{H}_\delta$ ,  $\text{H}_{5, 5'}$ ), 7.76 (d,  $J$  = 8.4 Hz, 1H;  $\text{H}_{13}$ ), 7.73 (d,  $J$  = 8.3 Hz, 1H;  $\text{H}_{13}$ ), 7.40 – 7.35 (m, 2H;  $\text{H}_\gamma$ ,  $\text{H}_{12}$ ), 7.30 (ddd,  $J$  = 16.7, 8.3, 1.0 Hz, 2H;  $\text{H}_{12}$ ,  $\text{H}_{11}$ ), 7.23 (dd,  $J$  = 8.3, 1.3 Hz, 1H;  $\text{H}_\alpha$ ), 7.18 (dd,  $J$  = 8.3, 1.3 Hz, 1H;  $\text{H}_\alpha$ ), 6.94 (t,  $J$  = 7.8 Hz, 1H;  $\text{H}_{11}$ ), 6.62 (d,  $J$  = 1.4 Hz, 1H;  $\text{H}_2$ ), 6.30 (d,  $J$  = 1.4 Hz, 1H;  $\text{H}_2$ ), 5.78 – 6.54 (m, 3H;  $2(\text{CH}(\text{CH}_3)_2)$ ,  $\text{H}_{10}$ ), 1.90 (dd,  $J$  = 9.5, 7.0 Hz, 3H;  $\text{CH}(\text{CH}_3)_2$ ), 1.83 (t,  $J$  = 6.9 Hz, 3H;  $\text{CH}(\text{CH}_3)_2$ ). <sup>13</sup>C NMR (126 MHz,  $\text{CD}_2\text{Cl}_2$ )  $\delta$  173.4, 162.8, 161.9, 153.7, 152.2, 150.5, 149.9, 141.0, 140.9, 139.73, 139.72, 139.44, 139.43, 138.41, 134.1, 133.9, 130.80, 130.78, 130.75, 130.6, 130.3, 130.13, 130.10, 130.08, 128.4, 128.0, 125.53, 125.49, 125.3, 125.2, 125.1, 124.4, 124.1, 123.6, 123.3, 123.2, 118.9, 118.84, 118.81, 118.30, 118.27, 118.24, 118.1, 115.4, 114.6,

114.0, 50.78, 50.77, 22.00, 21.96, 21.9, 21.8.  $^{19}\text{F}$  NMR (470 MHz,  $\text{CD}_2\text{Cl}_2$ )  $\delta$  -63.3, -63.5. HRMS (ESI) found  $m/z$  922.21583 calcd  $m/z$  922.21645 for  $\text{C}_{40}\text{H}_{33}\text{F}_6\text{IrN}_5\text{O}_2$  [M-H] $^+$ . Elemental Analysis calcd (%) for  $\text{C}_{40}\text{H}_{32}\text{F}_6\text{IrN}_5\text{O}_2 \cdot \text{H}_2\text{O}$ , C, 51.17; H, 3.65; N, 7.46, found C, 51.28; H, 3.76; N, 7.31.

**IrL<sup>6</sup>**<sub>2</sub>; Crude [Ir(L<sup>6</sup>)<sub>2</sub>( $\mu$ -Cl)]<sub>2</sub> (0.052 g 0.07 mmol), 2-picolinic acid (0.025 g 0.20 mmol),  $\text{Na}_2\text{CO}_3$  (0.022 g 0.020 mmol) and 2-ethoxyethanol/water 3:1 (10 mL).  $\text{SiO}_2$  ( $\text{CH}_2\text{Cl}_2/\text{CH}_3\text{OH}$ ) progressive increase of  $\text{CH}_3\text{OH}$  until 5%. Product isolated as a orange-yellowish powder (29 mg 49%).  $^1\text{H}$  NMR (500 MHz,  $\text{CD}_2\text{Cl}_2$ )  $\delta$  8.14 (d,  $J$  = 7.4 Hz, 1H;  $\text{H}_\alpha$ ), 8.00 – 7.94 (m, 1H;  $\text{H}_\beta$ ), 7.90 (d,  $J$  = 5.3 Hz, 1H;  $\text{H}_{10}$ ), 7.87 (td,  $J$  = 7.7, 1.5 Hz, 1H;  $\text{H}_6$ ), 7.73 (d,  $J$  = 8.8 Hz, 1H;  $\text{H}_5$ ), 7.71 (d,  $J$  = 8.8 Hz, 1H;  $\text{H}_5$ ), 7.67 – 7.62 (m, 2H;  $\text{H}_{13,13'}$ ), 7.36 – 7.32 (m, 1H;  $\text{H}_\nu$ ), 7.28 – 7.22 (m, 2H;  $\text{H}_{12,11}$ ), 7.17 (t,  $J$  = 7.8 Hz, 1H;  $\text{H}_{12'}$ ), 6.85 (t,  $J$  = 7.3 Hz, 1H;  $\text{H}_{11'}$ ), 6.56 (dd,  $J$  = 8.7, 2.7 Hz, 1H;  $\text{H}_4$ ), 6.51 (dd,  $J$  = 8.7, 2.7 Hz, 1H;  $\text{H}_4$ ), 5.94 (d,  $J$  = 2.6 Hz, 1H;  $\text{H}_2$ ), 5.70 (d,  $J$  = 2.7 Hz, 1H;  $\text{H}_2$ ), 5.69 (d,  $J$  = 2.8 Hz, 1H;  $\text{H}_{10'}$ ), 5.68 – 5.56 (m, 2H; 2( $\text{CH}(\text{CH}_3)_2$ )), 3.40 (s, 1H; Ph-OCH<sub>3</sub>), 3.32 (s, 1H; Ph-OCH<sub>3</sub>), 1.93 – 1.71 (m, 12H; 2( $\text{CH}(\text{CH}_3)_2$ )).  $^{13}\text{C}$  NMR (126 MHz,  $\text{CD}_2\text{Cl}_2$ )  $\delta$  173.4, 164.2, 163.1, 160.7, 160.4, 155.3, 153.9, 152.9, 149.8, 141.3, 141.2, 137.8, 134.0, 133.6, 128.5, 128.2, 128.0, 127.7, 126.9, 126.6, 124.2, 123.5, 122.7, 122.2, 119.6, 118.9, 117.6, 114.9, 113.9, 113.3, 108.0, 107.1, 54.9, 54.8, 50.1, 50.0, 21.9, 21.8, 21.7. HRMS (ESI) found  $m/z$  846.26255 calcd  $m/z$  846.26281 for  $\text{C}_{40}\text{H}_{39}\text{IrN}_5\text{O}_4$  [M-H] $^+$ . Elemental Analysis calcd (%) for  $\text{C}_{40}\text{H}_{38}\text{IrN}_5\text{O}_4$ , C, 56.85; H, 4.54; N, 8.29, found C, 56.71; H, 4.78; N, 8.44.

**IrL<sup>7</sup>**<sub>2</sub>; Crude [Ir(L<sup>7</sup>)<sub>2</sub>( $\mu$ -Cl)]<sub>2</sub> (0.111 g 0.11 mmol), 2-picolinic acid (0.042 g 0.34 mmol),  $\text{Na}_2\text{CO}_3$  (0.036 g 0.34 mmol) and 2-ethoxyethanol/water 3:1 (10 mL).  $\text{SiO}_2$  ( $\text{CH}_2\text{Cl}_2/\text{CH}_3\text{OH}$ ) progressive increase from 1% to 5% of  $\text{CH}_3\text{OH}$ . Product isolated as a bright yellow powder (90 mg 74%).  $^1\text{H}$  NMR (500 MHz,  $\text{CD}_2\text{Cl}_2$ )  $\delta$  8.41 (s, 1H;  $\text{H}_{10}$ ), 8.21 (d,  $J$  = 7.7 Hz, 1H;  $\text{H}_\alpha$ ), 7.98 – 7.91 (m, 2H;  $\text{H}_\beta, \delta$ ), 7.91 – 7.81 (m, 4H;  $\text{H}_{5,5'}$ ,  $\text{H}_{13,13'}$ ), 7.62 (d,  $J$  = 8.8 Hz, 1H;  $\text{H}_{12}$ ), 7.52 (d,  $J$  = 8.8 Hz, 1H;  $\text{H}_{12'}$ ), 7.47 – 7.40 (m, 1H;  $\text{H}_\nu$ ), 7.28 (d,  $J$  = 8.3 Hz, 1H;  $\text{H}_4$ ), 7.22 (d,  $J$  = 8.3 Hz, 1H;  $\text{H}_4$ ), 6.68 (s, 1H;  $\text{H}_2$ ), 6.29 (s, 1H;  $\text{H}_2$ ), 5.86 (s, 1H;  $\text{H}_{10'}$ ), 5.74 (hept,  $J$  = 13.8, 6.9 Hz, 2H; 2( $\text{CH}(\text{CH}_3)_2$ )), 2.04 – 1.75 (m, 12H; 2( $\text{CH}(\text{CH}_3)_2$ )).  $^{13}\text{C}$  NMR (126 MHz,  $\text{CD}_2\text{Cl}_2$ )  $\delta$  173.1, 165.1, 164.1, 153.6, 152.3, 151.0, 150.0, 140.6, 140.2, 138.9, 138.57, 138.56, 136.1, 135.9, 131.8, 131.5, 131.3, 131.2, 131.04, 131.02, 131.99, 130.96, 130.7, 130.5, 130.08, 130.05, 130.02, 130.00, 128.5, 128.4, 127.3, 127.0, 126.7, 126.4, 126.2, 125.8, 125.6, 125.3, 125.1, 123.7, 123.5, 123.1, 123.0, 120.95, 120.92, 120.90, 120.87, 120.39, 120.36, 120.34, 119.18, 119.15, 119.12, 118.67, 118.65, 118.62, 118.59, 115.82, 115.78, 115.75, 115.71, 115.27, 114.7, 112.91, 112.88, 112.84, 112.80, 51.30, 51.27, 22.0, 21.89, 21.86.  $^{19}\text{F}$  NMR (470 MHz,  $\text{CD}_2\text{Cl}_2$ )  $\delta$  -61.5, -61.8, -63.4, -63.6. HRMS (ESI) found  $m/z$  1058.19085 calcd  $m/z$  1058.19124 for  $\text{C}_{42}\text{H}_{31}\text{F}_{12}\text{IrN}_5\text{O}_2$  [M-H] $^+$ . Elemental Analysis calcd (%) for  $\text{C}_{42}\text{H}_{30}\text{F}_{12}\text{IrN}_5\text{O}_2$ , C, 47.72; H, 2.89; N, 6.63, found C, 47.55; H, 2.75; N, 6.87.

**IrL<sup>8</sup>**<sub>2</sub>; Crude [Ir(L<sup>8</sup>)<sub>2</sub>( $\mu$ -Cl)]<sub>2</sub> (0.054 g 0.07 mmol), 2-picolinic acid (0.024 g 0.20 mmol),  $\text{Na}_2\text{CO}_3$  (0.021 g 0.20 mmol) and 2-ethoxyethanol/water 3:1 (10 mL).  $\text{SiO}_2$  ( $\text{CH}_2\text{Cl}_2/\text{CH}_3\text{OH}$ ) progressive increase of  $\text{CH}_3\text{OH}$  until 5%. Product isolated as an orange powder (40 mg 67%).  $^1\text{H}$  NMR (500 MHz,  $\text{CD}_2\text{Cl}_2$ )  $\delta$  8.13

(d,  $J$  = 7.6, 1H;  $\text{H}_\alpha$ ), 7.86 (ddd,  $J$  = 8.9, 7.4, 5.4 Hz, 3H;  $\text{H}_\beta, \delta, \text{H}_{10}$ ), 7.66 (t,  $J$  = 8.3 Hz, 2H;  $\text{H}_{5,5'}$ ), 7.36 – 7.30 (m, 1H;  $\text{H}_\nu$ ), 7.11 (d,  $J$  = 2.2 Hz, 1H;  $\text{H}_{13}$ ), 7.08 (d,  $J$  = 2.2 Hz, 1H;  $\text{H}_{13'}$ ), 6.88 (dd,  $J$  = 9.0, 2.3 Hz, 1H;  $\text{H}_{11}$ ), 6.53 (dd,  $J$  = 8.7, 2.7 Hz, 1H;  $\text{H}_{11'}$ ), 6.51 – 6.46 (m, 2H,  $\text{H}_{4',4}$ ), 5.92 (d,  $J$  = 2.6 Hz, 1H;  $\text{H}_2$ ), 5.69 (t,  $J$  = 5.8 Hz, 1H;  $\text{H}_2$ ), 5.66 – 5.56 (m, 2H; 2( $\text{CH}(\text{CH}_3)_2$ )), 5.54 (d,  $J$  = 9.0 Hz, 1H;  $\text{H}_{10'}$ ), 3.85 (s, 3H; -OCH<sub>3</sub>), 3.82 (s, 3H; -OCH<sub>3</sub>), 3.42 (s, 3H; Ph-OCH<sub>3</sub>), 3.35 (s, 3H; Ph-OCH<sub>3</sub>), 1.87 – 1.75 (m, 12H; 2( $\text{CH}(\text{CH}_3)_2$ )).  $^{13}\text{C}$  NMR (126 MHz,  $\text{CD}_2\text{Cl}_2$ )  $\delta$  173.4, 163.7, 162.6, 160.4, 160.2, 156.5, 156.0, 154.7, 153.9, 152.2, 149.9, 137.7, 135.8, 134.7, 134.4, 128.9, 128.6, 128.0, 127.7, 126.4, 126.2, 119.5, 118.9, 118.0, 115.2, 112.1, 111.7, 107.7, 106.8, 98.5, 98.2, 56.50, 56.47, 55.0, 54.8, 49.9, 49.8, 21.75, 21.74, 21.6, 21.5. HRMS (ESI) found  $m/z$  906.28393 calcd  $m/z$  906.28397 for  $\text{C}_{42}\text{H}_{43}\text{IrN}_5\text{O}_6$  [M-H] $^+$ . Elemental Analysis calcd (%) for  $\text{C}_{42}\text{H}_{42}\text{IrN}_5\text{O}_6 \cdot \text{CH}_3\text{OH}$ , C, 55.11; H, 4.95; N, 7.47, found C, 55.23; H, 4.71; N, 7.58.

**IrL<sup>9</sup>**<sub>2</sub>; Crude [Ir(L<sup>9</sup>)<sub>2</sub>( $\mu$ -Cl)]<sub>2</sub> (0.044 g 0.05 mmol), 2-picolinic acid (0.018 g 0.14 mmol),  $\text{Na}_2\text{CO}_3$  (0.015 g 0.14 mmol) and 2-ethoxyethanol/water 3:1 (10 mL).  $\text{SiO}_2$  ( $\text{CH}_2\text{Cl}_2/\text{CH}_3\text{OH}$ ) progressive increase from 1% to 10% of  $\text{CH}_3\text{OH}$ . Product isolated as an orange powder (37 mg 63%).  $^1\text{H}$  NMR (500 MHz,  $\text{CD}_2\text{Cl}_2$ )  $\delta$  8.36 (s,  $J$  = 11.6 Hz, 1H;  $\text{H}_{10}$ ), 8.17 (d,  $J$  = 7.6 Hz, 1H;  $\text{H}_\alpha$ ), 7.94 (d,  $J$  = 5.3 Hz, 1H;  $\text{H}_6$ ), 7.91 (td,  $J$  = 7.7, 1.5 Hz, 1H;  $\text{H}_\beta$ ), 7.82 – 7.73 (m, 4H;  $\text{H}_{5,5'}$ ,  $\text{H}_{13,13'}$ ), 7.50 (dd,  $J$  = 8.7, 1.3 Hz, 1H;  $\text{H}_{12}$ ), 7.44 – 7.36 (m, 2H;  $\text{H}_\nu$ ,  $\text{H}_{12'}$ ), 6.61 (dd,  $J$  = 8.8, 2.6 Hz, 1H;  $\text{H}_4$ ), 6.56 (dd,  $J$  = 8.8, 2.6 Hz, 1H;  $\text{H}_4$ ), 6.00 (d,  $J$  = 2.6 Hz, 1H;  $\text{H}_2$ ), 5.79 (s, 1H;  $\text{H}_{10'}$ ), 5.75 – 5.62 (m, 3H; 2( $\text{CH}(\text{CH}_3)_2$ ),  $\text{H}_2$ ), 3.45 (s, 3H), 3.37 (s, 3H), 1.88 – 1.81 (m, 12H).  $^{13}\text{C}$  NMR (126 MHz,  $\text{CD}_2\text{Cl}_2$ )  $\delta$  173.1, 166.4, 165.3, 161.2, 161.0, 155.6, 153.9, 153.5, 149.9, 140.9, 140.7, 138.3, 136.1, 135.8, 128.3, 128.2, 128.1, 127.7, 127.6, 127.4, 127.3, 126.6, 126.4, 126.1, 126.0, 125.91, 125.87, 125.7, 125.5, 125.2, 124.0, 123.7, 121.8, 121.6, 119.9, 119.58, 119.56, 119.53, 119.07, 119.05, 119.02, 115.02, 114.99, 114.3, 113.9, 112.12, 112.09, 108.3, 107.4, 55.0, 54.9, 50.6, 50.5, 22.01, 21.97, 21.8, 21.7.  $^{19}\text{F}$  NMR (470 MHz,  $\text{CD}_2\text{Cl}_2$ )  $\delta$  -61.2, -61.5. HRMS (ESI) found  $m/z$  982.23679 calcd  $m/z$  982.23760 for  $\text{C}_{42}\text{H}_{37}\text{F}_6\text{IrN}_5\text{O}_4$  [M-H] $^+$ . Elemental Analysis calcd (%) for  $\text{C}_{42}\text{H}_{36}\text{F}_6\text{IrN}_5\text{O}_4$ , C, 51.42; H, 3.71; N, 7.14, found C, 51.56; H, 3.84; N, 7.25.

**IrL<sup>10</sup>**<sub>2</sub>; Crude [Ir(L<sup>10</sup>)<sub>2</sub>( $\mu$ -Cl)]<sub>2</sub> (0.043 g 0.05 mmol), 2-picolinic acid (0.018 g 0.15 mmol),  $\text{Na}_2\text{CO}_3$  (0.016 g 0.15 mmol) and 2-ethoxyethanol/water 3:1 (10 mL).  $\text{SiO}_2$  ( $\text{CH}_2\text{Cl}_2/\text{CH}_3\text{OH}$ ) progressive increase from 1% to 5% of  $\text{CH}_3\text{OH}$ . Product isolated as a bright yellow powder (27 mg 57%).  $^1\text{H}$  NMR (500 MHz,  $\text{CD}_2\text{Cl}_2$ )  $\delta$  8.17 (d,  $J$  = 7.3 Hz, 1H;  $\text{H}_\alpha$ ), 7.94 – 7.86 (m, 2H;  $\text{H}_{10}$ ,  $\text{H}_\beta$ ), 7.83 – 7.73 (m, 3H;  $\text{H}_6$ ,  $\text{H}_{5,5'}$ ), 7.36 (ddd,  $J$  = 7.5, 5.4, 1.5 Hz, 1H;  $\text{H}_\nu$ ), 7.21 (dd,  $J$  = 8.3, 1.3 Hz, 1H;  $\text{H}_4$ ), 7.18 – 7.11 (m, 3H;  $\text{H}_{18,13}$ ,  $\text{H}_4$ ), 6.95 (dd,  $J$  = 9.1, 2.3 Hz, 1H;  $\text{H}_{11}$ ), 6.60 (d,  $J$  = 1.4 Hz, 1H;  $\text{H}_2$ ), 6.56 (dd,  $J$  = 9.0, 2.3 Hz, 1H;  $\text{H}_{11'}$ ), 6.31 (d,  $J$  = 1.3 Hz, 1H;  $\text{H}_2$ ), 5.70 – 5.61 (m, 2H; 2( $\text{CH}(\text{CH}_3)_2$ )), 5.60 (d,  $J$  = 9.0 Hz, 1H;  $\text{H}_{10}$ ), 3.88 (s,  $J$  = 7.6 Hz, 3H; -OCH<sub>3</sub>), 3.85 (s, 3H; -OCH<sub>3</sub>), 1.88 (dd,  $J$  = 14.7, 7.0 Hz, 6H 2( $\text{CH}(\text{CH}_3)_2$ )), 1.81 (t,  $J$  = 7.1 Hz, 6H 2( $\text{CH}(\text{CH}_3)_2$ )).  $^{13}\text{C}$  NMR (126 MHz,  $\text{CD}_2\text{Cl}_2$ )  $\delta$  173.3, 162.2, 161.1, 157.4, 156.9, 153.7, 151.6, 149.9, 149.7, 140.0, 139.8, 139.7, 138.3, 135.5, 135.4, 135.0, 134.7, 130.62, 130.59, 130.56, 130.53, 130.4, 130.1, 130.04, 130.01, 129.98, 129.95, 129.89, 129.7, 128.3,

128.0, 125.6, 125.4, 127.0, 124.6, 123.4, 123.2, 118.78, 118.75, 118.72, 118.68, 118.22, 118.19, 118.16, 115.9, 113.7, 113.3, 98.4, 98.0, 56.5, 56.4, 50.5, 21.8, 21.70, 21.66, 21.60.  $^{19}\text{F}$  NMR (470 MHz,  $\text{CD}_2\text{Cl}_2$ )  $\delta$  -63.2, -63.3. HRMS (ESI) found  $m/z$  982.23673 calcd  $m/z$  982.23760 for  $\text{C}_{42}\text{H}_{37}\text{F}_6\text{IrN}_5\text{O}_4$   $[\text{M}-\text{H}]^+$ . Elemental Analysis calcd (%) for  $\text{C}_{42}\text{H}_{36}\text{F}_6\text{IrN}_5\text{O}_4$ , C, 51.42; H, 3.71; N, 7.14, found C, 51.49; H, 3.37; N, 6.99.

#### Computational details

Density Functional Theory (DFT) simulations have been performed using the Gaussian16 package.<sup>84</sup> Based on previous theoretical investigations conducted by some of us,<sup>85–88</sup> we considered the B3PW91 functional<sup>89–91</sup> in addition to the LanL2Dz basis set, which includes a pseudopotential to describe core electrons for large atoms together with polarization functions on C (d; 0.587), N (d; 0.736), O (d; 0.961), F (d; 1.577) Cl (d; 0.75) and Ir (f; 0.938).<sup>92–96</sup> The Polarizable Continuum Model (PCM)<sup>97,98</sup> was used to take into account solvent effects ( $\text{CH}_2\text{Cl}_2$ ). For computational savings, the -OMe and - $\text{N}^i\text{Pr}$  fragments were replaced by -OH and -NH groups. Geometry relaxations of the singlet (ground state) and triplet (excited state) states were performed and carefully checked by the calculation of the vibrational frequencies. The general Adiabatic Shift approach (AS)<sup>99</sup> was considered for estimating vibrational contributions into the computation of emission spectra.

All the simulated phosphorescence spectra were performed within the Franck-Condon approximation. The vibronic calculations were achieved enforcing a sum-overstates (time-independent) approach which implies a truncation of the summation over an infinite number of states. To limit the number of integrals to be taken into account, a class-based prescreening has been employed based on the work of Santoro and coworkers and as implemented into Gaussian. (F. Santoro, R. Improta, A. Lami, J. Bloino and V. Barone, *J. Chem. Phys.*, 2007, 126, 084509.

F. Santoro, A. Lami, R. Improta and V. Barone, *J. Chem. Phys.*, 2007, 126, 184102.

F. Santoro, A. Lami, R. Improta, J. Bloino and V. Barone, *J. Chem. Phys.*, 2008, 128, 224311)

In the present work, the following parameters were enforced:

$$C_1^{max} = 70, C_2^{max} = 70, N_I^{max} = 100 \times 10^8$$

The highest class state (maxbands tag) considered was 9.

Post-treatments were done using the Gaussview and VMS packages.<sup>100–102</sup> Horseshoe plots were realized using an in house Python code.

#### Conflicts of interest

There are no conflicts to declare.

#### Acknowledgements

The authors thank the CNRS and Université de Grenoble Alpes for their support. This work benefited from state aid managed by the National Research Agency under the “Investments for

the future” and frp, the “Investissements d’avenir” program bearing the reference ANR-15-IDEX-02. E.M.-V. was supported by the CONACYT program 707986. This work was partially supported by the CBH-EUR-GS (ANR-17-EURE-0003). For the purpose of Open Access, a CC-BY 4.0 public copyright licence (<https://creativecommons.org/licenses/by/4.0/>) has been applied by the authors to the present document and will be applied to all subsequent versions up to the Author Accepted Manuscript arising from this submission. The NanoBio ICMG (UAR 2607) is acknowledged for providing facilities for mass spectrometry (A. Durand, L. Fort, and R. Gueret), and single-crystal X-ray diffraction (N. Altounian).

#### Notes and references

- 1 D. J. Gaspar and E. Polikarpov, *OLED Fundamentals: Materials, Devices, and Processing of Organic Light-Emitting Diodes (1st ed.)*, CRC Press, CRC Press., 2015.
- 2 A. Sandström, P. Matyba and L. Edman, *Appl. Phys. Lett.*, 2010, **96**, 053303.
- 3 J. Kalinowski, V. Fattori, M. Cocchi and J. A. G. Williams, *Light-emitting devices based on organometallic platinum complexes as emitters*, Springer International Publishing, Berlin, Heidelberg Germany, Springer., 2011, vol. 255.
- 4 H. Yersin, in *Topics in Current Chemistry*, 2004, pp. 1–26.
- 5 H. Yersin, *Highly Efficient OLEDs with Phosphorescent Materials*, Wiley, 2007.
- 6 M. A. Baldo, M. E. Thompson and S. R. Forrest, *Nature*, 2000, **403**, 750–753.
- 7 A. F. Rausch, H. H. Homeier and H. Yersin, *Organometallic Pt(II) and Ir(III) Triplet Emitters for OLED Applications and the Role of Spin–Orbit Coupling: A Study Based on High-Resolution Optical Spectroscopy*, Berlin, Heidelberg Germany, Springer., 2010.
- 8 L. Silvestroni, G. Accorsi, N. Armaroli, V. Balzani, G. Bergamini, S. Campagna, F. Cardinali, C. Chiorboli, M. T. Indelli, N. A. P. Kane-Maguire, A. Listorti, F. Nastasi, F. Puntoriero and F. Scandola, *Photochemistry and Photophysics of Coordination Compounds I*, 2007, vol. 281.
- 9 A. Barbieri, F. Barigelletti, E. C.-C. Cheng, L. Flamigni, T. Gunnlaugsson, R. A. G. Kirgan, D. Kumaresan, J. P. Leonard, C. B. Nolan, D. P. Rillema, C. Sabatini, R. H. Schmehl, K. Shankar, F. Stomeo, B. P. Sullivan, S. Vaidya, B. Ventura and J. A. G. Williams, *Photochemistry and Photophysics of Coordination Compounds II*, Springer, Topics in current Chemistry, 2007.
- 10 D. H. Volman, G. S. Hammond, D. C. Neckers, M. Maestri, V. Balzani, C. Deuschel-Cornioley and A. Von Zelewsky, *Adv. Photochem.*, DOI:10.1002/9780470133484.ch1.
- 11 A. Barbieri, F. Barigelletti, E. C.-C. Cheng, L. Flamigni, T. Gunnlaugsson, R. A. Kirgan, D. Kumaresan, J. P. Leonard, C. B. Nolan, D. P. Rillema, C. Sabatini, R. H. Schmehl, K. Shankar, F. Stomeo, B. P. Sullivan, S. Vaidya, B. Ventura, J. A. G. Williams and V. W.-W. Yam, *Topics in Current Chemistry: Photochemistry and Photophysics of Coordination Compounds II*, Springer Berlin Heidelberg, 1980, vol. 7.

- 12 C. F. R. Mackenzie, L. Zhang, D. B. Cordes, A. M. Z. Slawin, I. D. W. Samuel and E. Zysman-Colman, *Adv. Opt. Mater.*, 2023, **11**, 1–14.
- 13 Y. Zhang and J. Qiao, *iScience*, 2021, **24**, 102858.
- 14 M. Mauro, *Chem. Commun.*, 2021, **57**, 5857–5870.
- 15 L. F. Gildea and J. A. G. Williams, in *Organic Light-Emitting Diodes (OLEDs)*, ed. A. Buckley, Woodhead Publishing, Sawston, UK, In Woodhead., 2013, pp. 77–113.
- 16 K. P. S. Zaroni, R. L. Coppo, R. C. Amaral and N. Y. Murakami Iha, *Dalton Trans.*, 2015, **44**, 14559–14573.
- 17 C. E. Housecroft and E. C. Constable, *Coord. Chem. Rev.*, 2017, **350**, 155–177.
- 18 E. Baranoff, J.-H. Yum, I. Jung, R. Vulcano, M. Grätzel and M. K. Nazeeruddin, *Chem. – An Asian J.*, 2010, **5**, 496–499.
- 19 H. Guo, S. Ji, W. W. Wu, J. Shao and J. Zhao, *Analyst*, 2010, **135**, 2832–2840.
- 20 S. Medina-Rodríguez, S. A. Denisov, Y. Cudré, L. Male, M. Marín-Suárez, A. Fernández-Gutiérrez, J. F. Fernández-Sánchez, A. Tron, G. Jonusauskas, N. D. McClenaghan and E. Baranoff, *Analyst*, 2016, **141**, 3090–3097.
- 21 J.-L. Fillaut, J. Andriès, R. D. Marwaha, P.-H. Lanoë, O. Lohio, L. Toupet and J. a. A. Gareth Williams, *J. Organomet. Chem.*, 2008, **693**, 228–234.
- 22 P.-H. Lanoë, J.-L. Fillaut, V. Guerchais, H. Le Bozec and J. a. G. Williams, *Eur. J. Inorg. Chem.*, 2011, **2011**, 1255–1259.
- 23 E. Ortega-Forte, S. Hernández-García, G. Viguera, P. Henarejos-Escudero, N. Cutillas, J. Ruiz and Fernando Gándia-Herrero, *Cell. Mol. Life Sci.*, 2022, **79**, 510.
- 24 J. Shen, T. W. Rees, L. Ji and H. Chao, *Coord. Chem. Rev.*, 2021, **443**, 214016.
- 25 C. Caporale and M. Massi, *Coord. Chem. Rev.*, 2018, **363**, 71–91.
- 26 C. Y.-S. Chung and V. W.-W. Yam, *Chemistry*, 2014, **20**, 13016–27.
- 27 T. Tu, W. Fang, X. Bao, X. Li and K. H. Dötz, *Angew. Chemie - Int. Ed.*, 2011, **50**, 6601–6605.
- 28 K. Li, T. Zou, Y. Chen, X. Guan and C. Che, *Chem. Eur. J.*, 2015, **21**, 7441–7453.
- 29 C. K. Prier, D. a Rankic and D. W. C. MacMillan, *Chem. Rev.*, 2013, **113**, 5322–5363.
- 30 H. L. B. S. Di Bella, C. Dragonetti, M. Pizzotti, D. Roberto, F. Tessore, R. Ugo, M. G. Humphrey, M. P. Cifuentes, M. Samoc, L. Murphy, J. A. G. Williams, Z. Liu, Z. Bian, C. Huang, N. C. Fletcher, M. C. Lagunas, V. Guerchais, *Top. Organomet. Chem.*, 2010, **37**, 179.
- 31 Z. Bian, M. P. Cifuentes, S. Di Bella, N. C. Fletcher, C. Dragonetti, V. Guerchais, C. Huang, M. G. Humphrey, M. C. Lagunas, J. A. G. Le Bozec, Hubert Williams, Z. Liu, L. Murphy, M. Pizzotti, R. M. S. Dominique A., F. Tessore and R. Ugo, *Molecular Organometallic Materials for Optics*, Springer., 2011, vol. 33.
- 32 G. Lu, L. Gu, S. Li, H.-B. Han, X. Wang, C. Zhou, J.-J. Lu and L. Zhou, *New J. Chem.*, 2023, 18603–18609.
- 33 Y. Tamura, Y. Hisamatsu, S. Kumar, T. Itoh, K. Sato, R. Kuroda and S. Aoki, *Inorg. Chem.*, 2017, **56**, 812–833.
- 34 M. Lepeltier, B. Graff, J. Lalevée, G. Wantz, M. Ibrahim-Ouali, D. Gigmes and F. Dumur, *Org. Electron. physics*, *Mater. Appl.*, 2016, **37**, 24–34.
- 35 Y. Hisamatsu, S. Kumar and S. Aoki, *Inorg. Chem.*, 2017, **56**, 886–899.
- 36 T. Sajoto, P. I. Djurovich, A. B. Tamayo, J. Oxgaard, W. A. Goddard and M. E. Thompson, *J. Am. Chem. Soc.*, 2009, **131**, 9813–9822.
- 37 P. J. Hay, *J. Phys. Chem. A*, 2002, **106**, 1634–1641.
- 38 A. J. Lees, *Comments Inorg. Chem. A J. Crit. Discuss. Curr. Lit.*, 1995, **17**, 319–346.
- 39 R. D. Costa, E. Ortí, H. J. Bolink, S. Graber, S. Schaffner, M. Neuburger, C. E. Housecroft and E. C. Constable, *Adv. Funct. Mater.*, 2009, **19**, 3456–3463.
- 40 A. F. Henwood and E. Zysman-Colman, *Top. Curr. Chem.*, DOI:10.1007/s41061-016-0036-0.
- 41 L. Flamigni, A. Barbieri, C. Sabatini, B. Ventura and F. Barigelletti, in *Photochemistry and Photophysics of Coordination Compounds II*, 2007, pp. 143–203.
- 42 P. A. Scattergood, A. M. Ranieri, L. Charalambou, A. Comia, D. A. W. Ross, C. R. Rice, S. J. O. Hardman, J.-L. Heully, I. M. Dixon, M. Massi, F. Alary and P. I. P. Elliott, *Inorg. Chem.*, 2020, **59**, 1785–180.
- 43 Z.-J. Gao, T.-H. Yeh, J.-J. Xu, C.-C. Lee, A. Chowdhury, B.-C. Wang, S.-W. Liu and C.-H. Chen, *ACS Omega*, 2020, **5**, 10553–10561.
- 44 D. Chen, W.-Z. He, H.-S. Liao, Y.-X. Hu, D.-D. Xie, B.-Y. Wang, H.-J. Chi, Y.-L. Lv, X. Zhu and X. Li, *Org. Electron.*, 2023, **113**, 106715.
- 45 Z. Ge, T. Hayakawa, S. Ando, M. Ueda, T. Akiike, H. Miyamoto, T. Kajita and M. Kakimoto, *Chem. Mater.*, 2008, **20**, 2532–2537.
- 46 J. H. Zhao, Y. X. Hu, H. Y. Lu, Y. L. Lü and X. Li, *Org. Electron.*, 2017, **41**, 56–72.
- 47 J. F. Lemonnier, L. Guénee, C. Beuchat, T. A. Wesolowski, P. Mukherjee, D. H. Waldeck, K. A. Gogick, S. Petoud and C. Piguet, *J. Am. Chem. Soc.*, 2011, **133**, 16219–16234.
- 48 N. M. Shavaleev, S. V. Eliseeva, R. Scopelliti and J. C. G. Bünzli, *Chem. Eur. J.*, 2009, **15**, 10790–10802.
- 49 J.-H. Zhao, Y.-X. Hu, Y. Dong, X. Xia, H.-J. Chi, G.-Y. Xiao, X. Li and D.-Y. Zhang, *New J. Chem.*, 2017, **41**, 1973–1979.
- 50 W. S. Huang, J. T. Lin, C. H. Chien, Y. T. Tao, S. S. Sun and Y. S. Wen, *Chem. Mater.*, 2004, **16**, 2480–2488.
- 51 J. Jayabharathi, K. Jayamoorthy and V. Thanikachalam, *J. Organomet. Chem.*, 2014, **761**, 74–83.
- 52 Y. Jiao, M. Li, N. Wang, T. Lu, L. Zhou, Y. Huang, Z. Lu, D. Luo and X. Pu, *J. Mater. Chem. C*, 2016, **4**, 4269–4277.
- 53 H. Cao, H. Sun, Y. Yin, X. Wen, G. Shan, Z. Su, R. Zhong, W. Xie, P. Li and D. Zhu, *J. Mater. Chem. C*, 2014, **2**, 2150–2159.
- 54 X. Wei, J. Peng, J. Cheng, M. Xie, Z. Lu, C. Li and Y. Cao, *Adv. Funct. Mater.*, 2007, **17**, 3319–3325.
- 55 G. Li, Y. Wu, G. Shan, W. Che, D. Zhu, B. Song, L. Yan, Z. Su and M. R. Bryce, *Chem. Commun.*, 2014, **50**, 6977–6980.
- 56 X. Ouyang, D. Chen, S. Zeng, X. Zhang, S. Su and Z. Ge, *J. Mater. Chem.*, 2012, **22**, 23005–23011.
- 57 H. T. Cao, L. Ding, J. Yu, G. G. Shan, T. Wang, H. Z. Sun, Y. Gao, W. F. Xie and Z. M. Su, *Dyes Pigments*, 2019, **160**, 119–127.

- 58 J. X. Cai, T. L. Ye, X. F. Fan, C. M. Han, H. Xu, L. L. Wang, D. G. Ma, Y. Lin and P. F. Yan, *J. Mater. Chem.*, 2011, **21**, 15405–15416.
- 59 L. Han, D. Zhang, Y. Zhou, Y. Yang, H. Y. Woo, F. Bai and R. Yang, *Dyes Pigments*, 2013, **99**, 1010–1015.
- 60 T. Yu, F. Yang, X. Chen, W. Su and Y. Zhao, *New J. Chem.*, 2017, **41**, 2046–2054.
- 61 H.-T. T. Mao, C.-X. X. Zang, G.-G. G. Shan, H.-Z. Z. Sun, W.-F. F. Xie and Z.-M. M. Su, *Inorg. Chem.*, 2017, **56**, 9979–9987.
- 62 S. V. Tatarin, P. Kalle, I. V. Taydakov, E. A. Varaksina, V. M. Korshunov and S. I. Bezzubov, *Dalton Trans.*, 2021, **50**, 6889–6900.
- 63 E. Martínez-Vollbert, C. Philouze, I. Gautier-Luneau, Y. Moreau, P.-H. Lanoë and F. Loiseau, *Phys. Chem. Chem. Phys.*, 2021, **23**, 24789–24800.
- 64 E. Martínez-Vollbert, C. Ciambrone, W. Lafargue-Dit-Hauret, C. Latouche, F. Loiseau and P.-H. Lanoë, *Inorg. Chem.*, 2022, **61**, 3033–3049.
- 65 T.-R. Chen, P.-C. Liu, H.-P. Lee, F.-S. Wu and K. H.-C. Chen, *Eur. J. Inorg. Chem.*, 2017, **2017**, 2023–2031.
- 66 D. G. Congrave, Y. ting Hsu, A. S. Batsanov, A. Beeby and M. R. Bryce, *Organometallics*, 2017, **36**, 981–993.
- 67 F. O. Garces, K. Dedeian, N. L. Keder and R. J. Watts, *Acta Crystallogr., Sect. C Cryst. Struct. Commun.*, 1993, **49**, 1117.
- 68 M. Nonoyama, *Bull. Chem. Soc. Jpn.*, 1974, **47**, 767.
- 69 K. J. Suhr, L. D. Bastatas, Y. Shen, L. A. Mitchell, G. A. Frazier, D. W. Taylor, J. D. Slinker and B. J. Holliday, *Dalton Trans.*, 2016, **45**, 17807–17823.
- 70 K. J. Suhr, L. D. Bastatas, Y. Shen, L. A. Mitchell, B. J. Holliday and J. D. Slinker, *ACS Appl. Mater. Interfaces*, 2016, **8**, 8888–8892.
- 71 M. Martínez-Alonso, J. Cerdá, C. Momblona, A. Pertegás, J. M. Junquera-Hernández, A. Heras, A. M. Rodríguez, G. Espino, H. Bolink and E. Ortí, *Inorg. Chem.*, 2017, **56**, 10298–10310.
- 72 K. A. Phillips, T. M. Stonelake, K. Chen, Y. Hou, J. Zhao, S. J. Coles, P. N. Horton, S. J. Keane, E. C. Stokes, I. A. Fallis, A. J. Hallett, S. P. O’Kell, J. M. Beames and S. J. A. Pope, *Chem. Eur. J.*, 2018, **24**, 8577–8588.
- 73 G. A. Jeffrey, *An Introduction to Hydrogen Bonding*, Oxford University Press, Oxford, 1997.
- 74 T. Steiner, *Angew. Chemie - Int. Ed.*, 2002, **41**, 48–76.
- 75 E. Baranoff and B. F. E. Curchod, *Dalton Trans.*, 2015, **44**, 8318–8329.
- 76 S. Neukermans, F. Vorobjov, T. Kenis, R. De Wolf, J. Hereijgers and T. Breugelmanns, *Electrochim. Acta*, , DOI:10.1016/j.electacta.2019.135484.
- 77 J. Frey, B. F. E. Curchod, R. Scopelliti, I. Tavernelli, U. Rothlisberger, M. K. Nazeeruddin and E. Baranoff, *Dalton Trans.*, 2014, **43**, 5667–5679.
- 78 J. C. Deaton and F. N. Castellano, in *Iridium(III) in Optoelectronic and Photonics Applications*, 2017, pp. 1–69.
- 79 Y. You and S. Y. Park, *Dalton Trans.*, 2009, 1267–1282.
- 80 G. A. Crosby, *Acc. Chem. Res.*, 1975, **8**, 231–238.
- 81 E. Baranoff, B. F. E. Curchod, F. Monti, F. Steimer, G. Accorsi, I. Tavernelli, U. Rothlisberger, R. Scopelliti, M. Grätzel and M. K. Nazeeruddin, *Inorg. Chem.*, 2012, **51**, 799–811.
- 82 S. Lamansky, P. Djurovich, D. Murphy, F. Abdel-Razzaq, R. Kwong, I. Tsyba, M. Bortz, B. Mui, R. Bau and M. E. Thompson, *Inorg. Chem.*, 2001, **40**, 1704–1711.
- 83 A. Juris, V. Balzani, F. Barigelletti, S. Campagna, P. Belser and A. von Zelewsky, *Coord. Chem. Rev.*, 1988, **84**, 85–277.
- 84 D. J. Frisch, M. J.; Trucks, G. W.; Schlegel, H. B.; Scuseria, G. E.; Robb, M. A.; Cheeseman, J. R.; Scalmani, G.; Barone, V.; Petersson, G. A.; Nakatsuji, H.; Li, X.; Caricato, M.; Marenich, A. V.; Bloino, J.; Janesko, B. G.; Gomperts, R.; Mennucci, B.; Hratch, 2016.
- 85 F. Vazart and C. Latouche, *Theor. Chem. Acc.*, 2015, **134**, 144.
- 86 C. Latouche, F. Palazzetti, D. Skouteris and V. Barone, *J. Chem. Theory Comput.*, 2014, **10**, 4565–4573.
- 87 C. Latouche, A. Baiardi and V. Barone, *J. Phys. Chem. B*, 2015, **119**, 7253–7257.
- 88 C. Latouche, D. Skouteris, F. Palazzetti and V. Barone, *J. Chem. Theory Comput.*, 2015, **11**, 3281–3289.
- 89 J. P. Perdew, K. Burke and Y. Wang, *Phys. Rev. B*, 1996, **54**, 16533–16539.
- 90 J. P. Perdew, *Phys. Rev. B*, 1986, **33**, 8822–8824.
- 91 A. D. Becke, *J. Chem. Phys.*, 1993, **98**, 5648–5652.
- 92 T. H. Dunning and P. J. Hay, ed. H. F. Schaefer, Springer US, Boston, MA, 1977, pp. 1–27.
- 93 W. R. Wadt and P. J. Hay, *J. Chem. Phys.*, 1985, **82**, 284–298.
- 94 P. J. Hay and W. R. Wadt, *J. Chem. Phys.*, 1985, **82**, 299–310.
- 95 P. J. Hay and W. R. Wadt, *J. Chem. Phys.*, 1985, **82**, 270–283.
- 96 R. Schira and C. Latouche, *Dalton Trans.*, 2021, **50**, 746–753.
- 97 R. C. Benedetta Mennucci, *Continuum Solvation Models in Chemical Physics: From Theory to Applications*, Wiley, Wiley., 2008.
- 98 B. Mennucci, J. Tomasi, R. Cammi, J. R. Cheeseman, M. J. Frisch, F. J. Devlin, S. Gabriel and P. J. Stephens, *J. Phys. Chem. A*, 2002, **106**, 6102–6113.
- 99 J. Bloino, M. Biczysko, F. Santoro and V. Barone, *J. Chem. Theory Comput.*, 2010, **6**, 1256–1274.
- 100 D. Licari, A. Baiardi, M. Biczysko, F. Egidi, C. Latouche and V. Barone, *J. Comput. Chem.*, 2015, **36**, 321–334.
- 101 V. Barone, *WIREs Comput. Mol. Sci.*, 2016, **6**, 86–110.
- 102 J. M. Dennington, R.; Keith, T. A.; Millam, 2019.